Journal of Molecular Structure 1218 (2020) 128454

Contents lists available at ScienceDirect

Journal of Molecular Structure

journal homepage: http://www.elsevier.com/locate/molstruc

# FTIR, Raman and DFT studies on 2-[4-(4-ethylbenzamido)phenyl] benzothiazole and 2-[4-(4-nitrobenzamido)phenyl]benzothiazole supported by differential scanning calorimetry

Ozan Unsalan [a, *], Hatice Arı [b], Cisem Altunayar-Unsalan [c], Kayhan Bolelli [d], Mustafa Boyukata [e], Ismail Yalcin [d]

[a] Ege University, Faculty of Science, Department of Physics, 35100, Bornova, Izmir, Turkey
[b] Yozgat Bozok University, Faculty of Art and Sciences, Chemistry Department, 66200, Yozgat, Turkey
[c] Ege University, Central Research Testing and Analysis Laboratory Research and Application Center, 35100, Bornova, Izmir, Turkey
[d] Ankara University, Faculty of Pharmacy, Department of Pharmaceutical Chemistry, Tandoğan, 06100, Ankara, Turkey
[e] Yozgat Bozok University, Faculty of Art & Sciences, Physics Department, 66200 Yozgat, Turkey

ARTICLE INFO

*Article history:*
Received 30 April 2020
Received in revised form
13 May 2020
Accepted 13 May 2020
Available online 16 May 2020

*Keywords:*
2-[4-(4-Ethylbenzamido)phenyl] benzothiazole
2-[4-(4-Nitrobenzamido)phenyl] benzothiazole
Raman
FTIR
DSC
DFT
drug likeness

ABSTRACT

Molecular structures and vibrational wavenumbers of 2-[4-(4-ethylbenzamido)phenyl]benzothiazole (BSN-009) and 2-[4-(4-nitrobenzamido)phenyl]benzothiazole (BSN-011) were determined by quantum chemical calculations, Infrared and Raman spectroscopic techniques. Vibrational modes were assigned by potential energy distributions (PED). Potential energy scan and conformational analysis were performed. Energy gap, ionization potential, electron affinity and electronegativity descriptors have been obtained from frontier molecular orbitals (HOMO and LUMO). Molecular electrostatic potential (MEP) surfaces have also been plotted for predicting the chemical reactivity of both compounds. Additionally, Mulliken atomic charges were discussed. All calculations were performed by Density Functional Theory (DFT) with B3LYP exchange correlation functional and 6−311++G(d,p) basis set. Moreover, based on the drug likeliness descriptors and bioactivity scores of these compounds, it was found that BSN-011 could be a good drug candidate. By using Differential Scanning Calorimetry (DSC), melting points of the compounds were obtained and the purities were calculated with van't Hoff equation.

© 2020 Elsevier B.V. All rights reserved.

## 1. Introduction

Heterocyclic compounds have been an interesting field in medicinal chemistry. A number of heterocyclic derivatives containing sulfur and nitrogen atom serve as a unique scaffolds for experimental drug design [1]. In the last decades, the microbial resistance has developed consequently a substantial medical need for new classes of antibacterial agents are in extreme demand, despite progress in public health care, hospital care and availability of powerful antibiotics [2]. Benzothiazoles are fused member rings, which contain the heterocycles bearing thiazole, showing numerous biological activities such as antimicrobial [3−10], topical carbonic anhydrase inhibitor [11], anticancer [12−21], anthelmintic [22], a cyclooxygenase inhibitor [23], antitubercular [24,25] and anti-diabetic [26] activities. Currently, synthesized benzothiazole containing compound, lysylamide of 2-(4-amino-3-methylphenyl)-5-fluorobenzothiazole had been tested for phase 1 clinical evaluation as an antitumor agent [14]. The synthesis of several 2-substitutedbenzothiazole derivatives as the antimicrobial agents has been previously reported [10,27−29]. In these studies, according to Yildiz-Oren et al. [10], the synthesized compounds were found to have inhibitory effect with minimum inhibitory concentration (MIC) value of 3.12−50 μg/ml against some of Gram-positive bacteria, Gram-negative bacteria and *Candida albicans* as yeast. Among the tested compounds, 2-(phenoxymethyl)benzothiazole was found as the most active derivative at a MIC value of 3.12 μg/ml against the tested *Staphylococcus aureus* [10]. Furthermore, according to Bolelli et al., the synthesized benzothiazole derivatives were *in vitro* tested for antibacterial activity against Gram-negative

* Corresponding author. Tel.: +90 2323112380.
*E-mail address:* physicistozan@gmail.com (O. Unsalan).

https://doi.org/10.1016/j.molstruc.2020.128454
0022-2860/© 2020 Elsevier B.V. All rights reserved.

bacteria, Gram-positive bacteria, and the antifungal activity as yeast. 2-[4-(4-Methoxyphenylacetamido)phenyl]benzothiazole was found the most active at a MIC value of 6.25 μg/ml against the tested *Pseudomonas aeruginosa* isolate [27].

For more than two decades, a great number of publications [30–39] deal with the quantum chemistry calculations have been applied on many compounds and these calculations play an important role in understanding the action mechanism of molecules, especially when they are candidates for potential drugs. Indeed, there are many studies which reveal new compounds and their structures by various spectroscopic, particularly Infrared and Raman spectroscopy, and structural studies. For example, in a work combining these two vibrational spectroscopic techniques together with molecular modelling study, an anticonvulsant agent was elucidated in order to better understand the epilepsy disease [40]. An anti-cancer drug, Combretastatin A-4 was also investigated by Density Functional Theory (DFT) and Surface Enhanced Raman Spectroscopy (SERS) technique and it was found out that this drug has two non-identical conformations [41]. Five platinum-based drugs, cisplatin, carboplatin, nedaplatin, oxaliplatin and heptaplatin were investigated by Infrared and Raman spectroscopy techniques and similarities and differences between their electronic structures were compared in order to better understand their nature. Authors also calculated harmonic vibrational spectra for dimers of these drugs except heptaplatin and showed that harmonic dimer vibrational spectra of cisplatin and nedaplatin were in better agreement with experiment than anharmonic computations of the monomers [42]. Vibrational properties of antiepileptic drug topiramate were studied by Fourier Transform Infrared (FTIR), Fourier Transform Raman (FT-Raman), X-Ray Diffraction (XRD) and DFT methods and observed bands were tentatively assigned for crystalline topiramate [43]. On the other hand, conformational analysis gives detailed information of various orientations of compounds and these conformations take place in their activity profiles. Conformational analysis and both experimental and theoretical computational study performed on borreverine, antimalarial natural product, revealed that this compound has two lowest energy conformers indeed confirmed by the observed bands in their Raman spectra [44].

Differential Scanning Calorimetry (DSC) is a sensitive technique to investigate the thermotropic properties of drugs as well as many different compounds. Recently, it has been utilized to determine drugs' purity, type of binding interaction, drugs' stability, conformation and polymorphism. For example, an antiparasitic drug praziquantel and its interaction with calcium carbonate was studied by DSC technique and it was shown that praziquantel prefers *anti* conformation rather than *syn* conformation and this multiconformational preference was also confirmed with the Infrared spectrum of the compound [45]. In a paper which investigates the polymorphism of Anti-HIV drug Efavirenz, polymorphs of this drug were compared by DSC together with complementary vibrational spectroscopic techniques and it was shown that one certain polymorph can be an excellent candidate for pharmaceutical formulations [46]. Dehydration, melting and crystallization profiles of carbamazepine (CBZ) were discussed in detail by DSC in terms of CBZ's polymorphs III and I and a detailed thermal pathway for the decomposition of CBZ were proposed. Authors also showed that the melting point of CBZ near temperatures of 200 °C indicated that Form I is the most stable [47]. In another study, thermal behavior of antihypertensive drug doxazosin mesilate was investigated by using DSC and the degree of purity of this drug was found to be similar as obtained by High Performance Liquid Chromatography (HPLC) [48]. Furthermore, in order to characterize and evaluate the biological activity of an anti-inflammatory drug meloxicam, DSC was used for the thermal analysis and melting points of two different polymorphs of meloxicam were observed at 260.12 and 261.50 °C for Form I and III, respectively [49].

In spite there are many efforts on drug design for clinical use, only a few drugs appeared as successful clinical use. Thus, in order to design novel and potentially active compounds as good candidate drugs, it is highly crucial to investigate their electronic structures and further reveal their molecular mechanism of interaction. Although there are numerous studies on benzothiazole derivatives investigated by quantum chemical calculations [37,50–57] due to their biological importance, there are still lack of studies on 2-[4-(4-ethylbenzamido)phenyl]benzothiazole (BSN-009) and 2-[4-(4-nitrobenzamido)phenyl]benzothiazole (BSN-011) (Fig. 1) in the literature to the best of our knowledge. For this reason, the main purpose of this research is to further investigate molecular structures of the title compounds by various analytical techniques to evaluate their potentials to be used as new drugs. Here, we report detailed vibrational spectroscopic (FTIR and Raman), calorimetric and DFT studies on BSN-009 and BSN-011 for giving any new perspectives for future studies, for the first time. Conformational analyses, (Highest Occupied Molecular Orbitals (HOMO) and Lowest Unoccupied Molecular Orbitals (LUMO)) and Molecular Electrostatic Potential (MEP) results were also reported for both compounds.

## 2. Experiments and theoretical methods

### 2.1. Fourier Transform Infrared spectroscopy

Approximately 5–10 mg solid powder samples of each compounds were placed on the diamond crystal of Attenuated Total Reflection (ATR) of the PerkinElmer Spectrum Two FTIR spectrometer (PerkinElmer Inc., Waltham, MA, USA) equipped with deuterium triglycide sulphide (DTGS) detector. All spectra were recorded in the range of 4000-400 $cm^{-1}$ with an average of 32 scans and spectral resolution of 1 $cm^{-1}$. All experiments were carried out at ambient temperature. The spectra were corrected from water and carbon dioxide contributions. ATR diamond crystal was cleaned with ultra-pure isopropyl alcohol prior to each sample and a background spectrum was taken by recording a clean and dry ATR crystal against air. The spectra were analyzed using PerkinElmer Spectrum Version 10.5.4. software (PerkinElmer Inc., Waltham, MA, USA).

### 2.2. Raman spectroscopy

Approximately 5–10 mg solid powder samples of each compounds were used to record Raman spectra on Renishaw InVia Raman spectrometer equipped with 785 nm red laser excitation line in the 4000-100 $cm^{-1}$ region with 0.6 $cm^{-1}$ resolution with a diode laser of 3.1 μm estimated laser spot size. Magnification was 50× *via* microscope. Slit aperture was 20 μm and 32 accumulations for each measurement were applied. For the calibration of the Raman spectrometer, silicon wafer (520.7 ± 0.5 $cm^{-1}$) was used. Detector was cooled to −70 °C thermoelectrically by peltier. CCDs are suitable for analysis of the inherently weak Raman signal and give the best possible sensitivity, uniformity and noise characteristics. The power of the incident laser requires to be low enough to avoid overheating and possible degradation.

### 2.3. Differential Scanning Calorimetry

Approximately 1.5 mg of samples from both compounds were encapsulated in standard aluminum hermetic DSC pans. Empty aluminum standard hermetic DSC pan was used as a reference pan for each sample separately. TA Q20 DSC (TA Instruments Inc., New

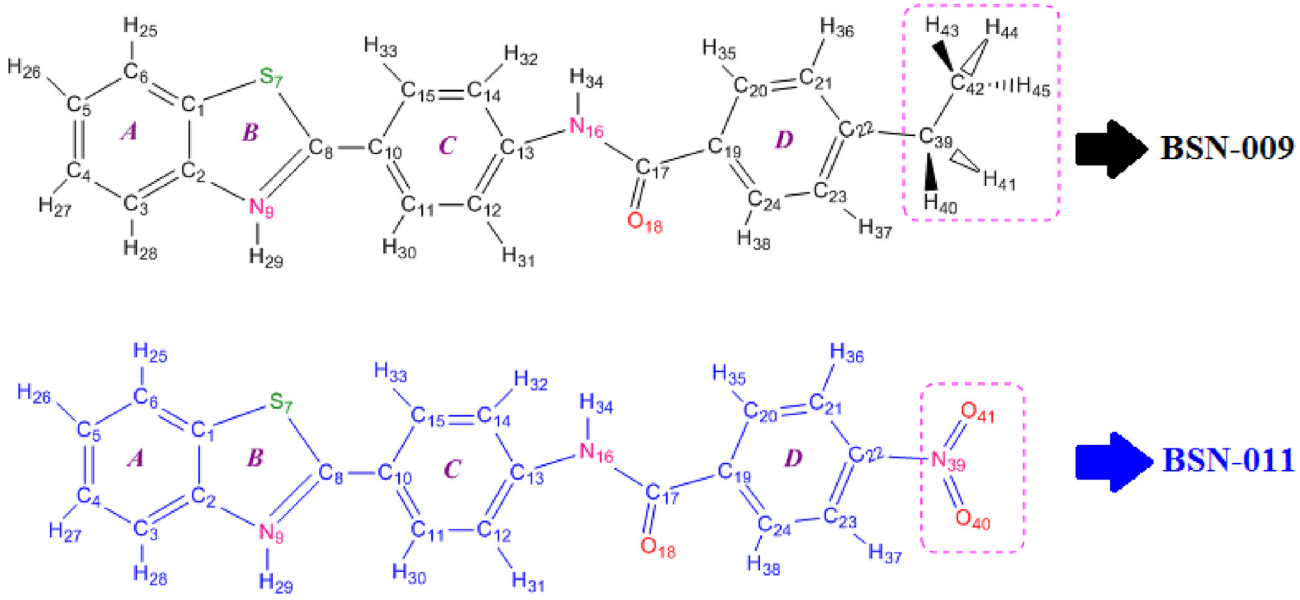


**Fig. 1.** Molecular structures of BSN-009 and BSN-011.

Castle, Delaware, USA) instrument was used with heating rates of 10 °C/min starting from 0 °C to 500 °C in nitrogen atmosphere with a flow rate of 50 mL/min. The DSC data were analyzed using Universal V4.5A TA Instruments software.

In a system which contains impurities, van't Hoff equation approximately holds and allows the purity value to be calculated as follows:

$$T_f = T_0 - \left[\left(\frac{RT_0^2X}{\Delta H_f}\right)\frac{1}{F}\right]$$

where $T_f$ is the melting temperature of the sample, $T_0$ is the melting point of pure substance in Kelvin (K), R is the gas constant, $\Delta H_f$ is the heat of fusion, F is the fraction melted and X is the mole fraction of impurities [48]. This technique also facilitates the design of new potential drugs or provide improvements of existing compounds [58].

### 2.4. DFT theoretical calculations

All calculations on BSN-009 and BSN-011 were performed *via* Gaussian09 quantum chemistry software [59], using DFT/B3LYP functional with 6–311++G(d,p) basis set. Optimized geometries, HOMO-LUMO and MEP from output files of calculations were visualized with Gauss View 5.0 program [60]. Vibrational mode assignments were done using Potential Energy Distribution (PED) analysis implemented in VEDA4 [61] software. Obtained harmonic vibrational wavenumbers were scaled by a single factor of 0.9780 in order to overcome systematic shortcomings of the applied methodology. No double scale factors, different scale factors before and after approximately 1800 $cm^{-1}$, were used for any of calculations [31,33,34]. Theoretical calculations were used to simulate both IR and Raman spectra of both compounds.

## 3. Results

### 3.1. Theoretical studies

#### 3.1.1. Potential energy scan and conformational analyses

Atom numbering and the molecular structures of BSN-009 and BSN-011 were given together in Fig. 1 to make comparison. Rotations around the single bonds give rise to energy minima. The structures obtained from the minima are re-optimized and identical structures were eliminated to get possible conformational isomers of BSN-009 and BSN-011. Relaxed scans for the torsional angles of $\tau(S_7C_8C_{10}C_{11})$, $\tau(C_{12}C_{13}N_{16}C_{17})$, $\tau(C_{13}N_{16}C_{17}C_{19})$, $\tau(N_{16}C_{17}C_{19}C_{20})$, $\tau(C_{21}C_{22}C_{39}C_{42})$ and $\tau(C_{22}C_{39}C_{42}H_{43})$ for BSN-009 and $\tau(S_7C_8C_{10}C_{11})$, $\tau(C_{12}C_{13}N_{16}C_{17})$, $\tau(C_{13}N_{16}C_{17}C_{19})$, $\tau(N_{16}C_{17}C_{19}C_{20})$, and $\tau(C_{21}C_{22}N_{39}O_{40})$ for BSN-011, respectively were performed in 0–360° range in 4° increments using B3LYP/6–311++G(d,p) given in Fig. S1. In order to get the most stable conformers, the potential energy scan results were employed as in previous studies [60–62]. Six and four stable conformers were obtained for BSN-009 and BSN-011, respectively. These conformers were depicted in Fig. 2 and Fig. 3.

Total energies, relative energies and dipole moments for the conformers of BSN-009 and BSN-011 were given in Table 1. The structures in which the carbonyl oxygen of the benzamido group and the sulfur atom of the benzothiazole group are in *trans* conformer were obtained as the most stable conformers for the two compounds. The geometric parameters of the lowest energy conformers, BSN-009 (1) and BSN-011 (1), were tabulated in Table S1 and Table S2 (Supplementary Data), respectively.

#### 3.1.2. Molecular properties from orbital energies

Highest Occupied Molecular Orbitals (HOMO) and Lowest Unoccupied Molecular Orbitals (LUMO) and their energy gaps are quite informative parameters in quantum chemistry. HOMO represents donation ability of an electron, whereas LUMO is descriptive for electron acceptor ability [62]. In general, positive phase corresponds to red in color and negative to green. It is known that the HOMO energy ($E_{HOMO}$) is related to the ionization potential (IP), where given by equation IP = $-E_{HOMO}$ (Koopmans' theorem [63]) and LUMO energy ($E_{LUMO}$) has been used to estimate the electron affinity where defined as EA = $-E_{LUMO}$, then the average value of the energies is related to the electronegativity given by the equation $\chi = (IP + EA)/2$ as defined by Mulliken [64].

Calculated HOMO and LUMO energies, HOMO-LUMO energy gaps and some main descriptors for the conformers of both compounds were given in Table 2. The energy gap of BSN-009 (1) is greater than BSN-011 (1), while the ionization potential, electron

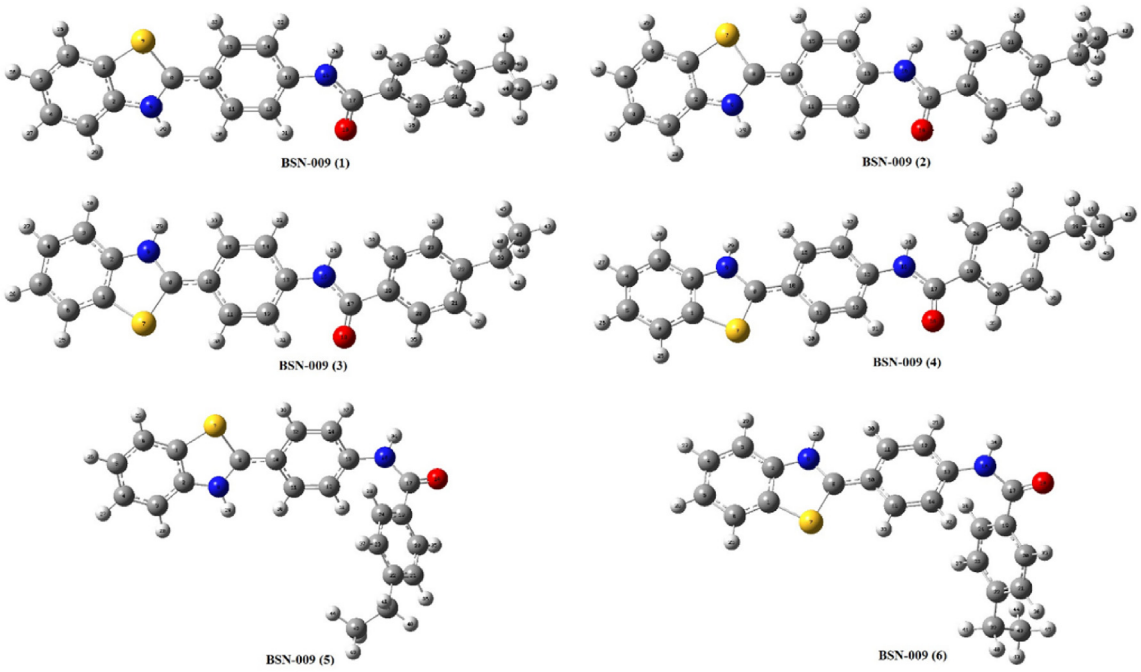


**Fig. 2.** The optimized conformer structures of BSN-009.

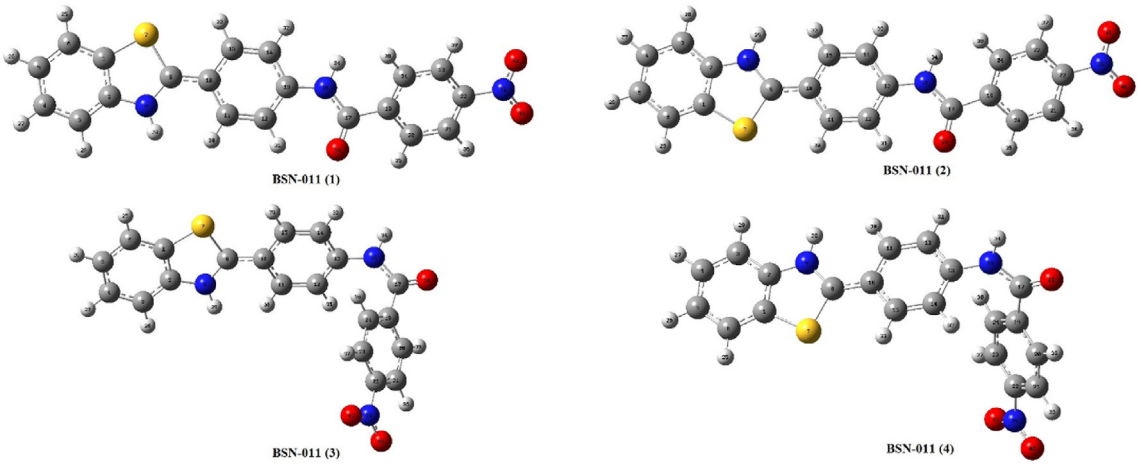


**Fig. 3.** The optimized conformer structures of BSN-011.

**Table 1**
Total energies, relative energies and dipole moments for the conformers of BSN-009 and BSN-011.

| Parameters | BSN-009 (1) | BSN-009 (2) | BSN-009 (3) | BSN-009 (4) | BSN-009 (5) | BSN-009 (6) |
|---|---|---|---|---|---|---|
| Energy (kcal/mol) | −899222.3401 | −899222.3237 | −899221.9187 | −899221.9057 | −899218.1461 | −899218.0267 |
| Rel. Energy (kcal/mol) | 0.0000 | 0.0164 | 0.4214 | 0.4344 | 4.1940 | 4.3134 |
| Dipole moment (Debye) | 1.7725 | 1.8340 | 5.0809 | 4.9768 | 6.1864 | 5.9572 |
| | **BSN-011 (1)** | **BSN-011 (2)** | **BSN-011 (3)** | **BSN-011 (4)** | | |
| Energy (kcal/mol) | −978232.3390 | −978231.9379 | −978228.3950 | −978228.1962 | | |
| Rel. Energy (kcal/mol) | 0.0000 | 0.4012 | 3.9441 | 4.1428 | | |
| Dipole moment (Debye) | 9.2845 | 9.9760 | 7.3040 | 8.8648 | | |

affinity and electronegativity values of BSN-011 (1) are higher than BSN-009(1). The molecular orbital shapes of BSN-009 (1) and BSN-011 (1) were presented in Fig. 4. As seen from the figure, the LUMO is mostly located over the entire molecule (especially nitrobenzene part for BSN-011), while the HOMO is more located on benzothiazole (A,B) part (mostly sulfur atom), phenyl (C) ring, N—H and C═O groups.

### 3.1.3. *Molecular Electrostatic Potential (MEP) analysis*

MEP surfaces visually indicate positive, negative and neutral

**Table 2**
Calculated molecular properties for the conformers of BSN-009 and BSN-011 from orbital energies (a.u.: atomic unit).

| Parameters | BSN-009 (1) | BSN-009 (2) | BSN-009 (3) | BSN-009 (4) | BSN-009 (5) | BSN-009 (6) |
|---|---|---|---|---|---|---|
| HOMO energy | −0.1356 | −0.1355 | −0.1993 | −0.1993 | −0.1988 | −0.1356 |
| LUMO energy | −0.0487 | −0.0489 | −0.1772 | −0.1772 | −0.1798 | −0.0487 |
| HOMO-LUMO energy gap | 0.0869 | 0.0866 | 0.0221 | 0.0221 | 0.0190 | 0.0870 |
| Ionization potential | 0.1356 | 0.1355 | 0.1993 | 0.1993 | 0.1988 | 0.1356 |
| Electron affinity | 0.0487 | 0.0489 | 0.1772 | 0.1772 | 0.1798 | 0.0487 |
| Electronegativity | 0.0921 | 0.0922 | 0.1882 | 0.1882 | 0.1893 | 0.0921 |
| | **BSN-011 (1)** | **BSN-011 (2)** | **BSN-011 (3)** | **BSN-011 (4)** | | |
| HOMO energy | −0.1475 | −0.1474 | −0.1536 | −0.1534 | | |
| LUMO energy | −0.1111 | −0.1111 | −0.1106 | −0.1092 | | |
| HOMO-LUMO energy gap | 0.0364 | 0.0363 | 0.0430 | 0.0442 | | |
| Ionization potential | 0.1475 | 0.1474 | 0.1536 | 0.1534 | | |
| Electron affinity | 0.1111 | 0.1111 | 0.1106 | 0.1092 | | |
| Electronegativity | 0.1293 | 0.1293 | 0.1321 | 0.1313 | | |

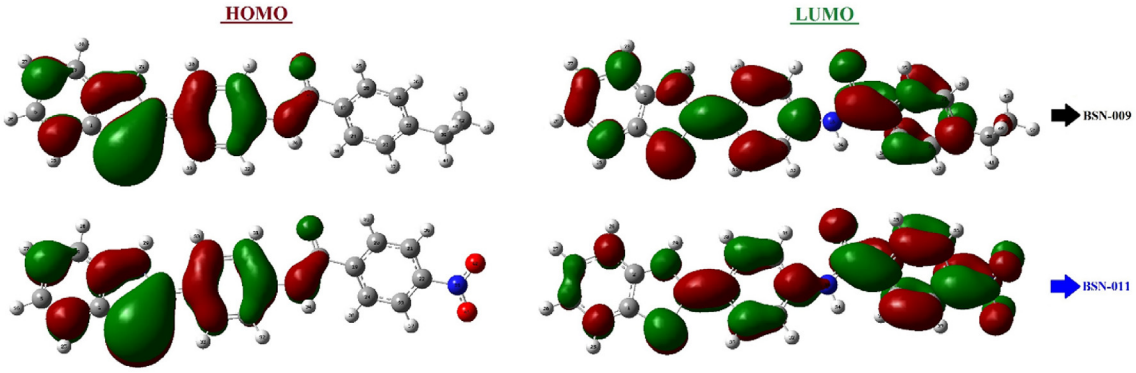


**Fig. 4.** The frontier molecular orbitals of BSN-009 (1) and BSN-011 (1).

electrostatic potential regions in terms of color grading as well as relative polarity of a molecule [65]. The different colors on the MEP surfaces of compound represent distinctive electrostatic potential regions (i.e., red for electron rich (partially negative charge); blue for electron deficient (partially positive charge); light blue for slightly electron deficient; yellow for slightly electron rich and green for neutral).

The MEP shapes of BSN-009 (1) and BSN-011 (1) were plotted in Fig. 5. The color codes of these maps are in the ranges between −0.131 a.u. (red) to 0.131 a.u. (blue) for BSN-009 and -0.152 a.u. (red) to 0.152 a.u. (blue) for BSN-011 calculated by DFT method. The electron deficient blue regions which are responsible for nucleophilic reactivity of the title compounds are located over N−H groups (mainly $N_9$−$H_{29}$). The electron rich red regions which are responsible for electronegativity of the two benzothiazole derivate are mostly located over the oxygen atoms. Red region count is higher in BSN-011 than BSN-009. This is because the electronegativity of the BSN-011, which has three oxygen atoms, is greater than BSN-009 which has only one oxygen atom (as seen in Table 2). The slightly electron deficient light blue regions for both compounds are located over thiazole ring. The slightly electron rich yellow region over the phenyl ring can be considered as the sites for electrophilic attacks.

### 3.1.4. Mulliken charges

Mulliken atomic charges are of importance in quantum chemical calculations since dipole moment, polarizability and electronic structure are highly affected by atomic charges. Calculated Mulliken charges were tabulated in Table 3. In order to further understand the Mulliken charges, a plot of charges versus atomic numbers was prepared in Fig. 6. According to the results, all hydrogen atoms in both compounds have positive charges and the hydrogen atom with the largest positive charge among them is $H_{29}$ (the sequence of hydrogen atoms with high positive charges; $H_{29}$> $H_{31}$> $H_{35}$> $H_{34}$). In addition, it is seen that $C_1$ (1.214) atom for BSN-009 and $C_{10}$ (1.051) atom for BSN-011 have higher Mulliken atomic charges than other positive atoms. Mulliken atomic charge values of $C_3$ (−0.657) for BSN-009 and $C_{22}$ (−0.624) atoms for BSN-011 were found to be highly negative values.

### 3.1.5. Drug likeliness properties and bioactivity scores

Very well-known Lipinski's rule of five [66–68] plays a major role in drug discovery and is of importance in estimating the bioavailability of compounds to reveal drug likeness properties. In our study, physicochemical properties of BSN-009 and BSN-011 were investigated by Molinspiration Cheminformatics online platform which calculates molecular properties and bioactivity score [69].

In order to begin Molinspiration work, DFT output files of both compounds were converted to standard SMILES codes by Open Babel software [70]. Afterwards, these SMILES codes were transferred to Molinspiration platform to draw their 2-dimensional structures and related properties were calculated. Corresponding SMILES codes and the drug likeness of both compounds in our work were presented in Table 4. As it is known that Lipinski's rule of five should satisfy following physicochemical characteristics: (i) clogP $\leq$ 5; (ii) Molecular weight (MW) $\leq$ 500 g/mol; (iii) number of hydrogen bond acceptors (HBA) (sum of N and O atoms) $\leq$ 10, (iv) number of hydrogen bond donors (HBD) (sum of OH and NH groups) $\leq$ 5. Other related criteria were added later by Veber et al. [71] are (v) number of rotatable bonds (nRotb) $\leq$ 10, (vi) topological polar surface area (TPSA) < 140 $Å^2$. According to Table 4, number of

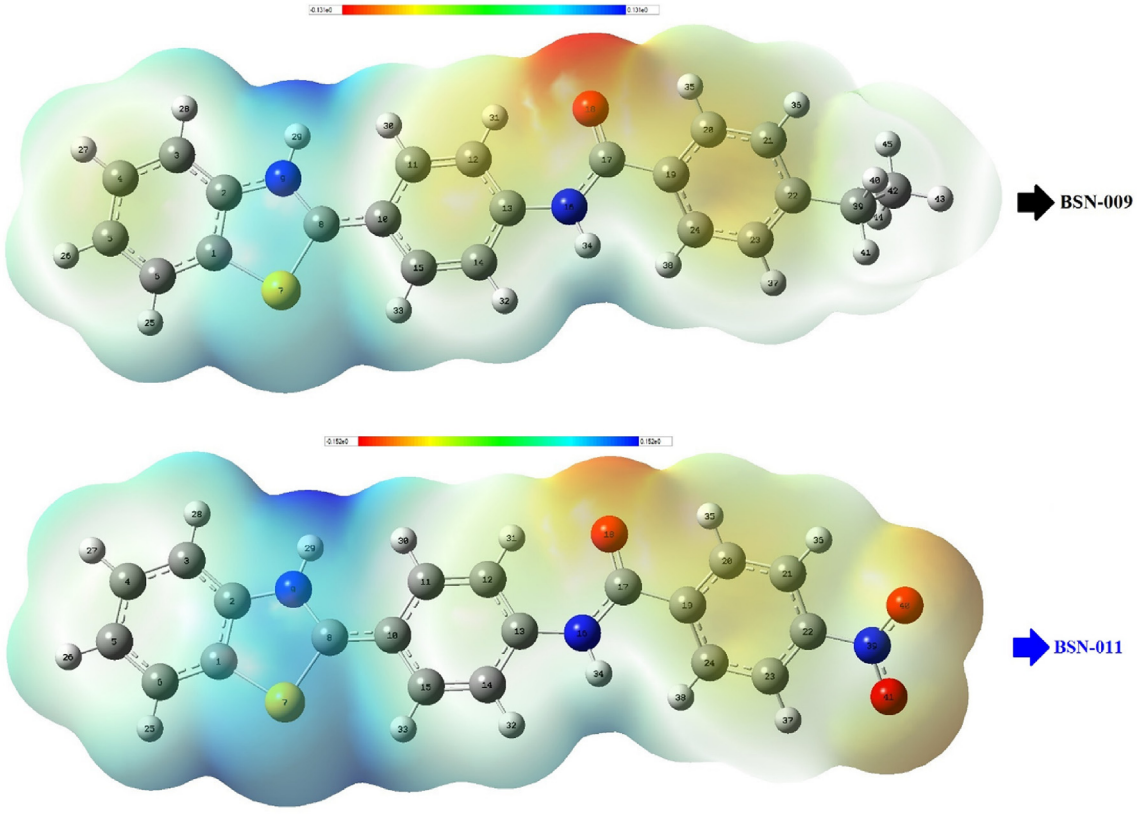


**Fig. 5.** The MEP maps of BSN-009 (1) and BSN-011 (1).

**Table 3**
Mulliken atomic charges of BSN-009 (1) and BSN-011 (1).

| BSN-009 (1) | | | | | |
|---|---|---|---|---|---|
| $C_1$ | 1.214 | $N_{16}$ | 0.080 | $H_{31}$ | 0.272 |
| $C_2$ | −0.334 | $C_{17}$ | −0.186 | $H_{32}$ | 0.151 |
| $C_3$ | −0.657 | $O_{18}$ | −0.296 | $H_{33}$ | 0.113 |
| $C_4$ | −0.369 | $C_{19}$ | 0.595 | $H_{34}$ | 0.203 |
| $C_5$ | −0.153 | $C_{20}$ | −0.139 | $H_{35}$ | 0.208 |
| $C_6$ | −0.308 | $C_{21}$ | −0.553 | $H_{36}$ | 0.170 |
| $S_7$ | −0.547 | $C_{22}$ | 0.832 | $H_{37}$ | 0.171 |
| $C_8$ | 0.211 | $C_{23}$ | −0.455 | $H_{38}$ | 0.139 |
| $N_9$ | 0.211 | $C_{24}$ | −0.500 | $C_{39}$ | −0.322 |
| $C_{10}$ | 1.025 | $H_{25}$ | 0.177 | $H_{40}$ | 0.151 |
| $C_{11}$ | −0.236 | $H_{26}$ | 0.163 | $H_{41}$ | 0.152 |
| $C_{12}$ | −0.356 | $H_{27}$ | 0.169 | $C_{42}$ | −0.626 |
| $C_{13}$ | −0.546 | $H_{28}$ | 0.147 | $H_{43}$ | 0.136 |
| $C_{14}$ | −0.325 | $H_{29}$ | 0.314 | $H_{44}$ | 0.145 |
| $C_{15}$ | −0.426 | $H_{30}$ | 0.039 | $H_{45}$ | 0.146 |
| **BSN-011 (1)** | | | | | |
| $C_1$ | 0.845 | $C_{15}$ | −0.449 | $H_{29}$ | 0.350 |
| $C_2$ | 0.113 | $N_{16}$ | 0.089 | $H_{30}$ | 0.020 |
| $C_3$ | −0.591 | $C_{17}$ | −0.103 | $H_{31}$ | 0.288 |
| $C_4$ | −0.359 | $O_{18}$ | −0.286 | $H_{32}$ | 0.157 |
| $C_5$ | −0.203 | $C_{19}$ | 0.761 | $H_{33}$ | 0.113 |
| $C_6$ | −0.350 | $C_{20}$ | −0.276 | $H_{34}$ | 0.201 |
| $S_7$ | −0.554 | $C_{21}$ | −0.090 | $H_{35}$ | 0.228 |
| $C_8$ | 0.242 | $C_{22}$ | −0.624 | $H_{36}$ | 0.251 |
| $N_9$ | 0.199 | $C_{23}$ | −0.014 | $H_{37}$ | 0.252 |
| $C_{10}$ | 1.051 | $C_{24}$ | −0.370 | $H_{38}$ | 0.162 |
| $C_{11}$ | −0.230 | $H_{25}$ | 0.184 | $N_{39}$ | −0.180 |
| $C_{12}$ | −0.340 | $H_{26}$ | 0.166 | $O_{40}$ | −0.008 |
| $C_{13}$ | −0.570 | $H_{27}$ | 0.174 | $O_{41}$ | −0.008 |
| $C_{14}$ | −0.384 | $H_{28}$ | 0.144 | | |

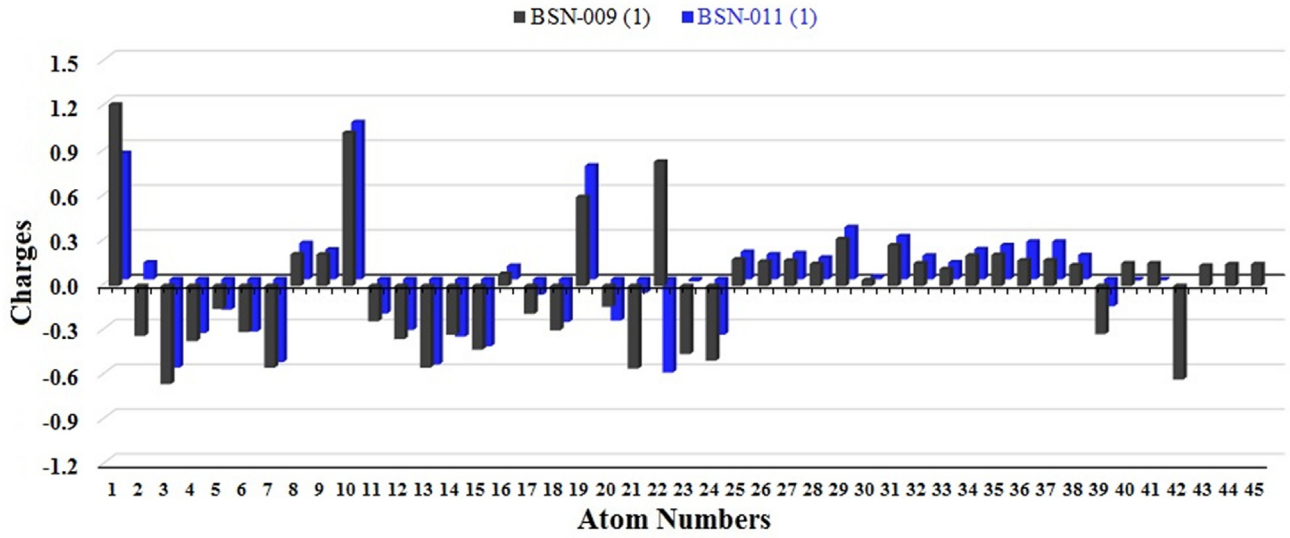


**Fig. 6.** Mulliken's plot of BSN-009 (1) and BSN-011 (1).

**Table 4**
Drug likeliness descriptor of BSN-009 and BSN-011 predicted from Molinspiration.

| Descriptors | BSN-009 | BSN-011 |
|---|---|---|
| Hydrogen bond donor (HBD) | 2 | 2 |
| Hydrogen bond acceptor (HBA) | 3 | 6 |
| Partition coefficient (Mi logP) | *5.42*[a] | 4.46 |
| Molecular weight (MW) | 359.47 | 376.42 |
| Topological polar surface area (TPSA) (Å$^2$) [74] | 41.12 | 86.95 |
| Number of atoms | 26 | 27 |
| Number of rotatable bonds [73] | 4 | 4 |
| Number of violations | *1*[a] | 0 |
| **Bioactivity Scores** | | |
| GPCR (G protein-coupled receptor) ligand | −0.23 | −0.36 |
| Ion channel modulator | −0.28 | −0.32 |
| Kinase inhibitor | −0.30 | −0.38 |
| Nuclear receptor ligand | −0.36 | −0.47 |
| Protease inhibitor | −0.15 | −0.28 |
| Enzyme inhibitor | −0.13 | −0.23 |

SMILES code for BSN-009: c12c(*cccc*1)N[C](S2)c1ccc(*cc*1)NC(=O)c1ccc(*cc*1)CC.
SMILES code for BSN-01: c12c(*cccc*1)N[C](S2)c1ccc(*cc*1)NC(=O)c1ccc(*cc*1)N(=O)=O.
[a] Partition coefficient violates rule of five and was given in *italics* on purpose.

HBD were found to be 2 (≤5) for both compounds. Number of HBA were found to be 3 and 6, for BSN-009 and BSN-011 (≤10), respectively. MW of BSN-009 was determined to be 359.47 g/mol, whereas 376.42 g/mol for BSN-011. van der Waals TPSA values obtained for BSN-009 and BSN-011 were 41.12 and 86.95 Å$^2$, respectively.

The bioactivity scores calculated for GPCR ligand, ion channel modulator, kinase inhibitor, nuclear receptor ligand, protease inhibitor and enzyme inhibitor were −0.23, −0.28, −0.30, −0.36, −0.15, −0.13 for BSN-009 and -0.36, −0.32, −0,38, −0.47, −0.28 and −0,23 for BSN-011 were also presented in Table 4.

### 3.2. Vibrational spectroscopic studies

Both compounds contain benzothiazole moieties, phenyl and benzamido parts and belong to $C_1$ point group symmetry. BSN-009 and BSN-011 consist of 45 and 41 atoms, respectively which have 129 and 117 normal modes of vibrations. In Table 5 and Table 6, computed vibrational wavenumbers were given with the experimental data for BSN-009 and BSN-011, respectively. In Fig. 7 and Fig. 8, experimental and calculated IR and Raman spectra of BSN-009 and BSN-011 were shown, respectively. Theoretical IR spectra for the compounds were scaled with 0.978. When comparing theoretical results with experimental ones, it should also be noted that only contributions more than 10% calculated by PED were evaluated for δCCH in-plane bending modes (Tables 5–6) (see Figs. 9 and 10).

#### 3.2.1. Stretching modes

*3.2.1.1. N–H stretching modes.* Vibrational wavenumber for N–H stretching mode of a benzothiazole derivate was reported at 3351 cm$^{-1}$ in our previous study [37]. Observed bands at 3347 and 3303 cm$^{-1}$ in IR spectra were assigned to $N_9$–$H_{29}$ and $N_{16}$–$H_{34}$ stretching modes which agrees with the literature. The $N_9$–$H_{29}$ stretching modes were calculated at 3568 cm$^{-1}$ and 3571 cm$^{-1}$ for BSN-009 and BSN-011, respectively. The $N_{16}$–$H_{34}$ stretching modes were calculated at 3544 cm$^{-1}$ and 3541 cm$^{-1}$ for BSN-009 and BSN-011, respectively. In Raman spectrum for BSN-009 and BSN-011, no Raman active bands were observed experimentally for this mode. Since the $N_9$–$H_{29}$ bond is shorter than the $N_{16}$–$H_{34}$ bond (as seen in Tables S1 and S2), the $N_9$–$H_{29}$ stretching vibrational mode were calculated at a higher frequency than the $N_{16}$–$H_{34}$ stretching mode.

*3.2.1.2. C–H stretching modes.* C–H stretching mode of aromatic ring occurs above 3000 cm$^{-1}$, whereas this mode for aliphatic chain occurs below 3000 cm$^{-1}$. Aromatic C–H stretching modes were observed at 3170, 3112 and 3054 cm$^{-1}$ in IR spectrum and calculated in the 3169-3077 cm$^{-1}$ region for BSN-009 in experiment. The aliphatic C–H stretching vibrations for ethyl group were calculated in the region 3028-2959 cm$^{-1}$ for BSN-009 in this study, while they were observed at 3032-2932 cm$^{-1}$. The aliphatic C–H stretching modes were observed at 3178, 3111 and 3065 cm$^{-1}$ in IR spectrum and calculated in the 3171-3080 cm$^{-1}$ for BSN-011 (Table 6). Unlike BSN-011, BSN-009, which has an ethyl group, has extra aliphatic C–H stretching modes ($\nu CH_2$ and $\nu CH_3$). C–H stretching modes for both compounds were not Raman active, thus these modes were not observed in corresponding Raman spectra and their Raman spectra were only presented in the region of 1700-100 cm$^{-1}$ in Figs. 7 and 8.

**Table 5**
Vibrational wavenumbers and assignments for BSN-009.

| No. | Raman | | Infrared | | | PED (%)[c,d] |
|---|---|---|---|---|---|---|
| | Exp.[a] | Calc.[a] | Exp. | Calc. | | |
| | | | | Unscld.[a] | Scld.[b,a] | |
| 1 | – | 3349 | 3347 | 3649 | 3568 | νNH(100) $N_9$–$H_{29}$ (B) |
| 2 | – | 3304 | 3303 | 3624 | 3544 | νNH(100) $N_{16}$–$H_{34}$ |
| 3 | – | 3169 | 3170 | 3240 | 3169 | νCH(98) $C_{12}$–$H_{31}$ (C) |
| 4 | – | – | – | 3199 | 3128 | νCH(96) $C_{20}$–$H_{35}$,$C_{21}$–$H_{36}$ (D) |
| 5 | – | – | – | 3197 | 3127 | νCH(92) $C_6$–$H_{25}$,$C_5$–$H_{26}$,$C_4$–$H_{27}$,$C_3$–$H_{28}$ (A) |
| 6 | – | 3115 | 3112 | 3186 | 3116 | νCH(96) $C_3$–$H_{28}$,$C_4$–$H_{27}$,$C_6$–$H_{25}$ (A) |
| 7 | – | – | – | 3178 | 3108 | νCH(99) $C_3$–$H_{28}$,$C_5$–$H_{26}$,$C_6$–$H_{25}$ (A) |
| 8 | – | 3106 | – | 3176 | 3106 | νCH(90) $C_{14}$–$H_{32}$,$C_{15}$–$H_{33}$ (C) |
| 9 | – | – | – | 3170 | 3100 | νCH(98) $C_{23}$–$H_{37}$,$C_{24}$–$H_{38}$ (D) |
| 10 | – | – | – | 3169 | 3100 | νCH(90) $C_3$–$H_{28}$,$C_4$–$H_{27}$,$C_6$–$H_{25}$,$C_5$–$H_{26}$ (A) |
| 11 | – | 3097 | – | 3162 | 3092 | νCH(98) $C_{11}$–$H_{30}$,$C_{12}$–$H_{31}$ (C) |
| 12 | – | 3088 | – | 3158 | 3089 | νCH(96) $C_{21}$–$H_{36}$,$C_{20}$–$H_{35}$ (D) |
| 13 | – | – | – | 3152 | 3083 | νCH(100) $C_{23}$–$H_{37}$,$C_{24}$–$H_{38}$ (D) |
| 14 | – | 3052 | 3054 | 3146 | 3077 | νCH(90) $C_{14}$–$H_{32}$,$C_{15}$–$H_{33}$ (C) |
| 15 | – | 3034 | 3032 | 3097 | 3028 | νCH(88) $C_{42}$–$H_{44}$,$C_{42}$–$H_{45}$ +νCH(11) $C_{39}$–$H_{40}$,$C_{39}$–$H_{41}$ |
| 16 | – | 3025 | 3032 | 3091 | 3023 | νCH(98) $C_{42}$–$H_{43}$,$C_{42}$–$H_{44}$,$C_{42}$–$H_{45}$ |
| 17 | – | 2998 | 3003 | 3058 | 2991 | νCH(88) $C_{39}$–$H_{40}$,$C_{39}$–$H_{41}$ +νCH(11) $C_{42}$–$H_{44}$,$C_{42}$–$H_{45}$ |
| 18 | – | 2962 | 2959 | 3027 | 2961 | νCH(95) $C_{39}$–$H_{40}$,$C_{39}$–$H_{41}$ |
| 19 | – | 2935 | 2932 | 3025 | 2959 | νCH(96) $C_{42}$–$H_{43}$,$C_{42}$–$H_{44}$,$C_{42}$–$H_{45}$ |
| 20 | 1658 | 1657 | 1655 | 1712 | 1675 | νCO(78) $C_{17}$=$O_{18}$ |
| 21 | 1607 | 1648 | – | 1648 | 1611 | νCC(62) $C_{20}$–$C_{21}$,$C_{21}$–$C_{22}$,$C_{19}$–$C_{20}$ (D) |
| 22 | – | 1594 | 1588 | 1627 | 1591 | νCC(50) $C_2$–$C_3$,$C_1$–$C_2$,$C_4$–$C_5$ (A) +δHNC(15) $H_{29}$–$N_9$–$C_8$ (B) |
| 23 | – | 1585 | 1588 | 1619 | 1584 | νCC(42) $C_{13}$–$C_{14}$,$C_{13}$–$C_{14}$,$C_{13}$–$C_{14}$ (C) |
| 24 | 1579 | 1576 | 1588 | 1616 | 1581 | νCC(55) $C_1$–$C_2$,$C_1$–$C_6$,$C_3$–$C_4$,$C_4$–$C_5$,$C_{11}$–$C_{12}$,$C_{14}$–$C_{15}$ (A,C) |
| 25 | 1562 | 1567 | 1570 | 1602 | 1567 | νCC(62) $C_{19}$–$C_{24}$,$C_{22}$–$C_{23}$,$C_{21}$–$C_{22}$,$C_{19}$–$C_{20}$ (D) |
| 26 | – | 1558 | 1558 | 1587 | 1552 | δHNC(45) $H_{34}$–$N_{16}$–$C_{13}$ +νCC(15) $C_{13}$–$C_{14}$ (C) |
| 27 | 1525 | 1513 | 1515 | 1558 | 1524 | νCC(36) $C_8$–$C_{10}$ +νNC(16) $N_9$–$C_8$ (B) +δHNC(11) $H_{29}$–$N_9$–$C_8$ (B) |
| 28 | 1498 | 1504 | 1503 | 1539 | 1505 | δHCC(46) $H_{38}$–$C_{24}$–$C_{19}$,$H_{35}$–$C_{20}$–$C_{19}$ (D) +νCC(11) $C_{19}$–$C_{20}$,$C_{19}$–$C_{24}$ (D) |
| 29 | 1483 | 1477 | 1479 | 1514 | 1481 | δHNC(26) $H_{34}$–$N_{16}$–$C_{13}$ +δHCC(25) $H_{33}$–$C_{15}$–$C_{10}$,$H_{32}$–$C_{14}$–$C_{13}$ (C) |
| 30 | – | 1477 | 1479 | 1510 | 1477 | δHCC(36) $H_{26}$–$C_5$–$C_4$,$H_{30}$–$C_{11}$–$C_{12}$ (A,C) + δHNC(13) $H_{29}$–$N_9$–$C_2$ (B) |
| 31 | – | – | 1479 | 1509 | 1475 | δHCH(76) $H_{40}$–$C_{39}$–$H_{41}$,$H_{44}$–$C_{42}$–$H_{45}$,$H_{43}$–$C_{42}$–$H_{45}$,$H_{43}$–$C_{42}$–$H_{44}$ |
| 32 | – | 1468 | 1456 | 1496 | 1463 | δHCH(78) $H_{43}$–$C_{42}$–$H_{44}$,$H_{43}$–$C_{42}$–$H_{45}$ |
| 33 | – | – | 1456 | 1495 | 1462 | δHCC(45) $H_{25}$–$C_6$–$C_5$,$H_{27}$–$C_4$–$C_3$, $H_{28}$–$C_3$–$C_2$ (A) +δCCC(11) $C_2$–$C_1$–$C_6$ (A) +νNC(10) $N_9$–$C_2$ |
| 34 | 1454 | 1459 | 1456 | 1491 | 1458 | δHCH(85) $H_{40}$–$C_{39}$–$H_{41}$,$H_{44}$–$C_{42}$–$H_{45}$ |
| 35 | 1435 | 1432 | 1434 | 1465 | 1433 | δHCC(45) $H_{26}$–$C_5$–$C_4$,$H_{27}$–$C_4$–$C_5$,$H_{31}$–$C_{12}$–$C_{11}$ (A,C) +δHNC(26) $H_{29}$–$N_9$–$C_2$,$H_{29}$–$N_9$–$C_8$ (B) |
| 36 | 1410 | 1414 | – | 1447 | 1415 | νCC(44) $C_{11}$–$C_{12}$,$C_{14}$–$C_{15}$ (C) +δHCC(11) $H_{32}$–$C_{14}$–$C_{15}$,$H_{33}$–$C_{15}$–$C_{14}$,$H_{30}$–$C_{11}$–$C_{12}$,$H_{31}$–$C_{12}$–$C_{11}$ (C) |
| 37 | – | 1405 | 1404 | 1438 | 1406 | νCC(48) $C_{23}$–$C_{24}$,$C_{20}$–$C_{21}$ (D) +δHCC(25) $H_{38}$–$C_{24}$–$C_{23}$,$H_{35}$–$C_{20}$–$C_{21}$ (D) |
| 38 | – | 1378 | 1377 | 1410 | 1379 | δHCC(66) $H_{44}$–$C_{42}$–$C_{39}$ +δHCH(15) $H_{43}$–$C_{42}$–$H_{45}$ |
| 39 | – | 1360 | 1353 | 1393 | 1363 | δHNC(19) $H_{29}$–$N_9$–$C_2$,$H_{29}$–$N_9$–$C_8$ (B) +δHCC(20) $H_{25}$–$C_6$–$C_1$,$H_{27}$–$C_4$–$C_5$ (A) +νCC(17) $C_8$–$C_{10}$ +νCN(17) $C_8$–$N_9$ |
| 40 | – | 1342 | 1342 | 1354 | 1324 | δHCC(28) $H_{35}$–$C_{20}$–$C_{19}$,$H_{38}$–$C_{24}$–$C_{19}$ (D) +δHCC(26) $H_{41}$–$C_{39}$–$C_{22}$ |
| 41 | – | 1333 | 1335 | 1350 | 1320 | δHCC(53) $H_{40}$–$C_{39}$–$C_{22}$,$H_{40}$–$C_{39}$–$C_{42}$ + δHCC(12) $H_{35}$–$C_{20}$–$C_{19}$,$H_{38}$–$C_{24}$–$C_{19}$ (D) |
| 42 | 1314 | 1315 | 1313 | 1342 | 1313 | δHCC (35) $H_{33}$–$C_{15}$–$C_{10}$, $H_{30}$–$C_{11}$–$C_{10}$, $H_{31}$–$C_{12}$–$C_{11}$ (C) +δNCC (27) $N_{16}$–$C_{13}$–$C_{14}$ |
| 43 | – | 1306 | 1313 | 1334 | 1304 | δHCC(46) $H_{38}$–$C_{24}$–$C_{19}$,$H_{36}$–$C_{21}$–$C_{22}$,$H_{37}$–$C_{23}$–$C_{24}$,$H_{35}$–$C_{20}$–$C_{21}$ (D) +νCC(14) $C_{21}$–$C_{22}$,$C_{23}$–$C_{24}$ (D) |
| 44 | – | – | 1313 | 1331 | 1302 | νCC(43) $C_1$–$C_2$,$C_1$–$C_6$,$C_4$–$C_5$,$C_2$–$C_3$,$C_5$–$C_6$ (A)+ νCC(19) $C_8$–$C_{10}$ +δHCC(10) $H_{26}$–$C_5$–$C_4$,$H_{28}$–$C_3$–$C_4$ (A) |
| 45 | – | 1297 | 1288 | 1327 | 1298 | νCN(42) $C_{13}$–$N_{16}$ +νCC(37) $C_{10}$–$C_{11}$,$C_{10}$–$C_{15}$,$C_{12}$–$C_{13}$,$C_{13}$–$C_{14}$ (C) + δHCC (11) $H_{37}$–$C_{23}$–$C_{24}$ (D) |
| 46 | – | 1252 | 1252 | 1285 | 1257 | νNC(29) $N_9$–$C_2$ (B) + δHCC(19) $H_{25}$–$C_6$–$C_1$ (A) + δNCC(12) $N_9$–$C_2$–$C_3$ +δHNC(11) $H_{29}$–$N_9$–$C_2$ (B) |
| 47 | 1249 | – | 1244 | 1277 | 1249 | δHNC(49) $H_{29}$–$N_9$–$C_8$ +δHCC(19) $H_{25}$–$C_6$–$C_1$,$H_{28}$–$C_3$–$C_2$ (A) +νNC(10) $N_9$–$C_2$ (B) |
| 48 | 1241 | 1243 | 1244 | 1271 | 1243 | δHCC(36) $H_{40}$–$C_{39}$–$C_{42}$,$H_{40}$–$C_{39}$–$C_{22}$ +δHCH(11) $H_{43}$–$C_{42}$–$H_{44}$,$H_{43}$–$C_{42}$–$H_{45}$ |
| 49 | – | 1234 | 1226 | 1267 | 1239 | νCN(31) $C_{13}$–$N_{16}$ +νCN(15) $C_2$–$N_9$ (B) +δHNC(12) $H_{29}$–$N_9$–$C_2$ (B) +νCC(10) $C_{17}$–$C_{19}$ (C) |
| 50 | 1228 | 1225 | 1226 | 1254 | 1227 | νCC(35) $C_{17}$–$C_{19}$ +νNC(13) $N_{16}$–$C_{17}$ +δHNC(12) $H_{34}$–$N_{16}$–$C_{13}$ +δHCC(10) $H_{36}$–$C_{21}$–$C_{20}$,$H_{31}$–$C_{12}$–$C_{11}$ (D,C) |
| 51 | 1198 | 1198 | 1199 | 1227 | 1200 | νCC(64) $C_{22}$–$C_{39}$,$C_{23}$–$C_{24}$ +δHCC(13) $H_{38}$–$C_{24}$–$C_{23}$,$H_{35}$–$C_{20}$–$C_{21}$ (D) |
| 52 | 1183 | 1189 | 1180 | 1215 | 1188 | δHCC(23) $H_{30}$–$C_{11}$–$C_{12}$, $H_{31}$–$C_{12}$–$C_{11}$, $H_{32}$–$C_{14}$–$C_{15}$ (B) + νNC(12) $N_9$–$C_8$ +δHNC(10) $H_{34}$–$N_{16}$–$C_{13}$ |
| 53 | – | 1180 | 1180 | 1207 | 1181 | δHCC(87) $H_{35}$–$C_{20}$–$C_{21}$,$H_{36}$–$C_{21}$–$C_{20}$,$H_{38}$–$C_{24}$–$C_{23}$, $H_{37}$–$C_{23}$–$C_{24}$ (D) |
| 54 | – | 1162 | 1158 | 1192 | 1165 | δHCC(36) $H_{33}$–$C_{15}$–$C_{14}$,$H_{32}$–$C_{14}$–$C_{15}$ (C)+ δNCC(14) $N_9$–$C_8$–$C_{10}$ |
| 55 | 1154 | 1153 | – | 1181 | 1155 | δHCC(65) $H_{26}$–$C_5$–$C_4$,$H_{27}$–$C_4$–$C_5$,$H_{25}$–$C_6$–$C_5$ (A) |
| 56 | 1123 | 1126 | 1130 | 1148 | 1123 | δHCC(25) $H_{32}$–$C_{14}$–$C_{15}$,$H_{33}$–$C_{15}$–$C_{14}$,$H_{31}$–$C_{12}$–$C_{11}$,$H_{30}$–$C_{11}$–$C_{12}$ (B) +δHNC (12) $H_{29}$–$N_9$–$C_8$ (B) |
| 57 | – | – | 1117 | 1144 | 1119 | δHCC(41) $H_{26}$–$C_5$–$C_4$,$H_{27}$–$C_4$–$C_5$,$H_{26}$–$C_5$–$C_6$ (A) +νSC(15) $C_1$–$S_7$ +νCC(10) $C_1$–$C_2$ |
| 58 | – | 1117 | 1105 | 1143 | 1118 | δHCC(43) $H_{37}$–$C_{23}$–$C_{22}$,$H_{36}$–$C_{21}$–$C_{22}$,$H_{35}$–$C_{20}$–$C_{19}$,$H_{38}$–$C_{24}$–$C_{19}$ (D) |
| 59 | – | 1090 | – | 1115 | 1091 | νNC(53) $N_{16}$–$C_{17}$ +δHCC(17) $H_{35}$–$C_{20}$–$C_{19}$,$H_{38}$–$C_{24}$–$C_{19}$ (D) +δCCC(16) $C_{17}$–$C_{19}$–$C_{20}$ |
| 60 | – | 1054 | 1053 | 1079 | 1055 | δHCC(42) $H_{43}$–$C_{42}$–$C_{39}$,$H_{44}$–$C_{42}$–$C_{39}$,$H_{45}$–$C_{42}$–$C_{39}$ |
| 61 | – | – | 1053 | 1074 | 1051 | νSC(49) $C_1$–$S_7$ (B) +νCC(12) $C_1$–$C_2$,$C_1$–$C_6$ (A) |
| 62 | 1048 | 1045 | 1053 | 1068 | 1044 | δHCH(35) $H_{43}$–$C_{42}$–$H_{44}$,$H_{43}$–$C_{42}$–$H_{45}$ +δHCC(19) $H_{40}$–$C_{39}$–$C_{22}$,$H_{41}$–$C_{39}$–$C_{22}$ |
| 63 | 1015 | 1018 | 1018 | 1042 | 1019 | δCCC(70) $C_3$–$C_4$–$C_5$,$C_4$–$C_5$–$C_6$ (A)+δHCC(12) $H_{28}$–$C_3$–$C_4$,$H_{24}$–$C_6$–$C_5$,$H_{26}$–$C_5$–$C_4$ (A) |
| 64 | 1015 | 1009 | 1012 | 1034 | 1012 | δCCC(72) $C_{19}$–$C_{20}$–$C_{21}$,$C_{20}$–$C_{21}$–$C_{22}$,$C_{22}$–$C_{23}$–$C_{24}$ (D) +δHCC(12) $H_{36}$–$C_{21}$–$C_{20}$,$H_{38}$–$C_{24}$–$C_{23}$ (D) |
| 65 | 985 | 982 | 987 | 1008 | 986 | δCCC(55) $C_{10}$–$C_{11}$–$C_{12}$,$C_{10}$–$C_{15}$–$C_{14}$ (C) +δHCC(14) $H_{33}$–$C_{15}$–$C_{14}$,$H_{31}$–$C_{12}$–$C_{11}$ (C) |
| 66 | 967 | 973 | 966 | 994 | 972 | γHCCC(80) $H_{35}$–$C_{20}$–$C_{21}$–$C_{22}$,$H_{36}$–$C_{21}$–$C_{20}$–$C_{19}$ out of H (D) |
| 67 | – | 946 | 947 | 970 | 949 | νCC(82) $C_{39}$–$C_{42}$ |
| 68 | – | – | 947 | 969 | 948 | γHCCC(75) $H_{31}$–$C_{12}$–$C_{11}$–$C_{10}$,$H_{30}$–$C_{11}$–$C_{12}$–$C_{13}$ out of H (C) |
| 69 | – | – | 947 | 966 | 945 | γHCCC(87) $H_{26}$–$C_5$–$C_4$–$C_3$,$H_{27}$–$C_4$–$C_3$–$C_2$ out of H (A) |
| 70 | – | – | 947 | 965 | 944 | γHCCC(79) $H_{38}$–$C_{24}$–$C_{19}$–$C_{20}$,$H_{37}$–$C_{23}$–$C_{22}$–$C_{21}$ out of H (D) |
| 71 | – | 937 | 937 | 961 | 939 | νSC(36) $S_7$–$C_8$ (B) +δHNC (19) $H_{29}$–$N_9$–$C_8$ (B) |

**Table 5** (*continued*)

| No. | Raman | | Infrared | | | PED (%)[c,d] |
|---|---|---|---|---|---|---|
| | Exp.[a] | Calc.[a] | Exp. | Calc. | | |
| | | | | Unscld.[a] | Scld.[b,a] | |
| 72 | 902 | 910 | 897 | 929 | 908 | γHCCC(78) $H_{33}$–$C_{15}$–$C_{10}$–$C_8$,$H_{32}$–$C_{14}$–$C_{13}$–$C_{12}$ out of H (C) |
| 73 | – | 901 | 897 | 922 | 902 | γHCCC(82) $H_{26}$–$C_5$–$C_4$–$C_3$,$H_{27}$–$C_4$–$C_5$–$C_6$, $H_{25}$–$C_6$–$C_1$–$S_7$, $H_{28}$–$C_3$–$C_2$–$N_9$ out of H (A) |
| 74 | – | 883 | – | 904 | 884 | δNCO(47) $N_{16}$–$C_{17}$–$O_{18}$ +δCNC(11) $C_{13}$–$N_{16}$–$C_{17}$ +νCC(10) $C_{17}$–$C_{19}$ +νNC(10) $N_{16}$–$C_{17}$ |
| 75 | 841 | | 855 | 867 | 848 | γHCCC(58) $H_{36}$–$C_{21}$–$C_{20}$–$C_{19}$,$H_{35}$–$C_{20}$–$C_{21}$–$C_{22}$ out of H (D) |
| 76 | 841 | 847 | 855 | 866 | 847 | δCCC(32) $C_4$–$C_5$–$C_6$ (A) +δCCC (10) $C_{10}$–$C_{11}$–$C_{12}$,$C_{10}$–$C_{15}$–$C_{14}$ (C) |
| 77 | – | 829 | 839 | 847 | 829 | γHCCC(65) $H_{35}$–$C_{20}$–$C_{19}$–$C_{17}$,$H_{36}$–$C_{21}$–$C_{22}$–$C_{39}$,$H_{38}$–$C_{24}$–$C_{19}$–$C_{17}$,$H_{37}$–$C_{23}$–$C_{22}$–$C_{39}$ out of H (D) |
| 78 | 823 | 820 | 822 | 837 | 818 | γHCCC(93) $H_{28}$–$C_3$–$C_2$–$C_1$,$H_{25}$–$C_6$–$C_1$–$C_2$,$H_{26}$–$C_5$–$C_6$–$C_1$,$H_{27}$–$C_4$–$C_3$–$C_2$ out of H (A) |
| 79 | – | 811 | – | 829 | 811 | νCN(22) $C_{13}$–$N_{16}$ +νCC(16) $C_{12}$–$C_{13}$,$C_{13}$–$C_{14}$ (C) +γHCCC(11) $H_{38}$–$C_{24}$–$C_{19}$–$C_{20}$,$H_{37}$–$C_{23}$–$C_{22}$–$C_{21}$ out of H (D) |
| 80 | 788 | 784 | 784 | 794 | 776 | τHCCH(58) $H_{40}$–$C_{39}$–$C_{42}$–$H_{44}$,$H_{41}$–$C_{39}$–$C_{42}$–$H_{45}$ |
| 81 | 771 | 775 | 770 | 793 | 775 | γHCCC(69) $H_{30}$–$C_{11}$–$C_{10}$–$C_8$,$H_{31}$–$C_{12}$–$C_{13}$–$N_{16}$,$H_{33}$–$C_{15}$–$C_{10}$–$C_8$,$H_{32}$–$C_{14}$–$C_{13}$–$N_{16}$ out of H (C) |
| 82 | 771 | – | 770 | 787 | 770 | γHCCC(57) $H_{30}$–$C_{11}$–$C_{10}$–$C_8$,$H_{31}$–$C_{12}$–$C_{13}$–$N_{16}$,$H_{33}$–$C_{15}$–$C_{10}$–$C_8$,$H_{32}$–$C_{14}$–$C_{13}$–$N_{16}$ out of H (C) |
| 83 | 771 | 766 | 770 | 785 | 768 | γHCCC(76) $H_{30}$–$C_{11}$–$C_{10}$–$C_8$,$H_{31}$–$C_{12}$–$C_{13}$–$N_{16}$,$H_{33}$–$C_{15}$–$C_{10}$–$C_8$,$H_{32}$–$C_{14}$–$C_{13}$–$N_{16}$ out of H (C) |
| 84 | – | 757 | 756 | 770 | 753 | γONCC(70) $O_{18}$–$N_{16}$–$C_{17}$–$C_{19}$ +τHCCC(10) $C_{24}$–$C_{20}$–$C_{19}$–$C_{17}$ (D) |
| 85 | 726 | 721 | 727 | 743 | 727 | γHCCC(89) $H_{25}$–$C_6$–$C_5$–$C_4$,$H_{27}$–$C_4$–$C_3$–$C_2$,$H_{28}$–$C_3$–$C_2$–$C_1$,$H_{26}$–$C_5$–$C_6$–$C_1$ out of H (A) |
| 86 | 710 | – | 698 | 713 | 697 | γCCCC(66) $C_{10}$–$C_{11}$–$C_{12}$–$C_{13}$,$C_{10}$–$C_{15}$–$C_{14}$–$C_{13}$,$C_3$–$C_2$–$C_1$–$C_6$ out of C (C,A) +γONCC(14) $O_{18}$–$N_{16}$–$C_{17}$–$C_{19}$ |
| 87 | – | 694 | 698 | 710 | 694 | νSC(46) $C_1$–$S_7$ +δCCC(25) $C_2$–$C_1$–$C_6$,$C_3$–$C_4$–$C_5$ (A) |
| 88 | – | – | 698 | 708 | 692 | γOCNC(52) $O_{18}$–$C_{19}$–$N_{16}$–$C_{17}$ +γHCCC(22) $H_{37}$–$C_{23}$–$C_{22}$–$C_{21}$,$H_{36}$–$C_{21}$–$C_{22}$–$C_{23}$ out of H (D) |
| 89 | 677 | 685 | – | 703 | 687 | τCCCC(78) $C_1$–$C_2$–$C_3$–$C_4$,$C_5$–$C_6$–$C_1$–$C_2$,$C_{10}$–$C_{11}$–$C_{12}$–$C_{13}$,$C_{10}$–$C_{15}$–$C_{14}$–$C_{13}$ (A,C) |
| 90 | – | 667 | – | 682 | 667 | νSC(37) $S_7$–$C_8$ +δNCC(15) $N_9$–$C_8$–$C_{10}$ |
| 91 | 652 | 649 | 648 | 656 | 642 | δCCN(30) $C_{12}$–$C_{13}$–$N_{16}$,$C_3$–$C_2$–$N_9$ +δCCC(16) $C_4$–$C_5$–$C_6$,$C_{11}$–$C_{12}$–$C_{13}$ (A,C) +δCNC(10) $C_2$–$N_9$–$C_8$ |
| 92 | – | – | 630 | 652 | 638 | δCCC(77) $C_{19}$–$C_{20}$–$C_{21}$,$C_{19}$–$C_{24}$–$C_{23}$ (D) |
| 93 | 629 | 631 | 623 | 642 | 628 | δCCC(63) $C_{10}$–$C_{11}$–$C_{12}$,$C_{10}$–$C_{15}$–$C_{14}$ (C) |
| 94 | – | 595 | 597 | 616 | 602 | δCCC(25) $C_{22}$–$C_{39}$–$C_{42}$,$C_{20}$–$C_{21}$–$C_{22}$,$C_{22}$–$C_{23}$–$C_{24}$ (C) +δCCC(12) $C_{23}$–$C_{22}$–$C_{21}$ (D) |
| 95 | – | 559 | 562 | 573 | 560 | γHNCC(57) $H_{34}$–$N_{16}$–$C_{13}$–$C_{12}$ out of N |
| 996 | 553 | 550 | 553 | 560 | 547 | γHNCC(60) $H_{34}$–$N_{16}$–$C_{13}$–$C_{12}$ out of N |
| 97 | 549 | 532 | – | 543 | 531 | τCCCC(80) $C_3$–$C_4$–$C_5$–$C_6$,$C_1$–$C_6$–$C_5$–$C_4$ (A) +γCCCN(11) $C_6$–$C_1$–$C_2$–$N_9$ (B) |
| 98 | 506 | 505 | 509 | 521 | 509 | τCCCC(21) $C_{19}$–$C_{20}$–$C_{21}$–$C_{22}$,$C_{19}$–$C_{24}$–$C_{23}$–$C_{22}$ (D) |
| 99 | – | 487 | 481 | 501 | 490 | γHCCC(65) $H_{30}$–$C_{11}$–$C_{10}$–$C_{15}$, $H_{31}$–$C_{12}$–$C_{11}$–$C_{10}$, $H_{32}$–$C_{14}$–$C_{15}$–$C_{10}$ out of H (C) |
| 100 | 468 | 469 | 469 | 497 | 486 | δCSC(52) $C_1$–$S_7$–$C_8$ (B) +δSCN(13) $S_7$–$C_8$–$N_9$ (B) |
| 101 | 458 | 451 | 451 | 473 | 462 | τCCCC(28) $C_{23}$–$C_{22}$–$C_{39}$–$C_{42}$ |
| 102 | 440 | 433 | 435 | 425 | 416 | τCCCC(48) $C_3$–$C_2$–$C_1$–$C_6$,$C_4$–$C_3$–$C_2$–$C_1$ (A) |
| 103 | – | 424 | 422 | 423 | 413 | τCCCC(61) $C_2$–$C_1$–$C_6$–$C_5$,$C_4$–$C_3$–$C_2$–$C_1$ (A) |
| 104 | 411 | 415 | 411 | 416 | 407 | τCCCC(82) $C_{22}$–$C_{21}$–$C_{20}$–$C_{19}$,$C_{20}$–$C_{21}$–$C_{22}$–$C_{23}$,$C_{10}$–$C_{15}$–$C_{14}$–$C_{13}$ (D,C) |
| 105 | – | 406 | 411 | 416 | 407 | τCCCC(86) $C_8$–$C_{10}$–$C_{15}$–$C_{14}$,$C_{10}$–$C_{15}$–$C_{14}$–$C_{13}$,$C_{22}$–$C_{21}$–$C_{20}$–$C_{19}$ (C,D) |
| 106 | – | 379 | – | 386 | 378 | γSCNC(22) $S_7$–$C_{10}$–$N_9$–$C_8$ +τCCNC(10) $C_{12}$–$C_{13}$–$N_{16}$–$C_{17}$ |
| 107 | – | 361 | – | 369 | 361 | δCCN(50) $C_{14}$–$C_{13}$–$N_{16}$ +δNCO(20) $N_{16}$–$C_{17}$–$O_{18}$ |
| 108 | – | 352 | – | 362 | 354 | δCCC(28) $C_{22}$–$C_{39}$–$C_{42}$,$C_{17}$–$C_{19}$–$C_{20}$,$C_{23}$–$C_{22}$–$C_{39}$ |
| 109 | – | 334 | – | 339 | 332 | τHCCC(44) $H_{43}$–$C_{42}$–$C_{39}$–$C_{22}$ |
| 110 | 308 | 307 | – | 313 | 306 | δCNC(16) $C_{13}$–$N_{16}$–$C_{17}$,$C_2$–$N_9$–$C_8$ +δCCC(12) $C_{17}$–$C_{19}$–$C_{24}$ +τHNCC(10) $H_{29}$–$N_9$–$C_2$–$C_1$ |
| 111 | 302 | 298 | – | 300 | 293 | τNCCC(39) $N_9$–$C_8$–$C_{10}$–$C_{15}$ +τHCCH(16) $H_{40}$–$C_{39}$–$C_{42}$–$H_{43}$ |
| 112 | 284 | 280 | – | 287 | 281 | τCNCC(10) $C_{13}$–$N_{16}$–$C_{17}$–$C_{19}$ +δCCC(10) $C_{17}$–$C_{19}$–$C_{20}$ |
| 113 | 256 | 262 | – | 268 | 262 | τHNCC(65) $H_{29}$–$N_9$–$C_2$–$C_1$ |
| 114 | – | 235 | – | 242 | 237 | τHNCC(18) $H_{29}$–$N_9$–$C_8$–$C_{10}$ + τHCCC(17) $H_{43}$–$C_{42}$–$C_{39}$–$C_{22}$ |
| 115 | – | 226 | – | 230 | 225 | τHCCC(22) $H_{43}$–$C_{42}$–$C_{39}$–$C_{22}$,$H_{45}$–$C_{42}$–$C_{39}$–$C_{22}$ +τHCCH(10) $H_{40}$–$C_{39}$–$C_{42}$–$H_{43}$ |
| 116 | 203 | 208 | – | 208 | 203 | τHCCC(13) $H_{43}$–$C_{42}$–$C_{39}$–$C_{22}$,$H_{45}$–$C_{42}$–$C_{39}$–$C_{22}$ +τHCCH(11) $H_{41}$–$C_{39}$–$C_{42}$–$H_{44}$ |
| 117 | – | 190 | – | 195 | 191 | τHCCC(30) $H_{43}$–$C_{42}$–$C_{39}$–$C_{22}$,$H_{45}$–$C_{42}$–$C_{39}$–$C_{22}$ +τHCCH(12) $H_{40}$–$C_{39}$–$C_{42}$–$H_{44}$ |
| 118 | – | 172 | – | 174 | 170 | τSCCH(71) $S_7$–$C_1$–$C_6$–$H_{25}$ +τNCCH(14) $N_9$–$C_2$–$C_3$–$H_{28}$ |
| 119 | 145 | 136 | – | 140 | 137 | τCCNC(10) $C_{14}$–$C_{13}$–$N_{16}$–$C_{17}$ |
| 120 | – | 118 | – | 125 | 122 | δCNC(41) $C_{13}$–$N_{16}$–$C_{17}$ +τCCNC(12) $C_{14}$–$C_{13}$–$N_{16}$–$C_{17}$ |
| 121 | – | 91 | – | 93 | 91 | τCCCN(19) $N_{16}$–$C_{17}$–$C_{19}$–$C_{24}$ +τCNCC(16) $C_2$–$N_9$–$C_8$–$C_{10}$ |
| 122 | – | – | – | 79 | 77 | τOCCC(36) $O_{18}$–$C_{17}$–$C_{19}$–$C_{24}$ +γCCNC(23) $C_{12}$–$C_{13}$–$N_{16}$–$C_{17}$ |
| 123 | – | 73 | – | 71 | 70 | γCNCC(16) $C_{13}$–$N_{16}$–$C_{17}$–$C_{19}$,$C_2$–$N_9$–$C_8$–$C_{10}$ +δCNC(14) $C_{13}$–$N_{16}$–$C_{17}$ |
| 124 | – | 55 | – | 51 | 50 | τCCCC(48) $C_{21}$–$C_{22}$–$C_{39}$–$C_{42}$ |
| 125 | – | 46 | – | 44 | 43 | τCNCC(39) $C_{12}$–$C_{13}$–$N_{16}$–$C_{17}$ +τCCNC(15) $C_{14}$–$C_{13}$–$N_{16}$–$C_{17}$ +τCCCC(14) $C_{21}$–$C_{22}$–$C_{39}$–$C_{42}$ |
| 126 | – | 37 | – | 36 | 35 | τCNCC(42) $C_2$–$N_9$–$C_8$–$C_{10}$,$C_{13}$–$N_{16}$–$C_{17}$–$C_{19}$ +τCCCC(16) $C_{21}$–$C_{22}$–$C_{39}$–$C_{42}$ |
| 127 | – | – | – | 33 | 32 | δCNC(32) $C_{13}$–$N_{16}$–$C_{17}$ +τCNCC(19) $C_2$–$N_9$–$C_8$–$C_{10}$ +τCCNC(17) $C_{14}$–$C_{13}$–$N_{16}$–$C_{17}$ |
| 128 | – | 28 | – | 25 | 25 | τCCNC(49) $C_{14}$–$C_{13}$–$N_{16}$–$C_{17}$ +τCNCC(24) $C_2$–$N_9$–$C_8$–$C_{10}$ +τCCCC(11) $C_{21}$–$C_{22}$–$C_{39}$–$C_{42}$ |
| 129 | – | 10 | – | 14 | 14 | τCNCC(49) $C_{13}$–$N_{16}$–$C_{17}$–$C_{19}$ +τCCNC(17) $C_2$–$N_9$–$C_8$–$C_{10}$ +τCCCC(13) $C_{17}$–$C_{19}$–$C_{24}$–$C_{23}$ |

[a] Exp.: Experimental, Calc.:Calculated, Unscld.:Unscaled, Scld.:Scaled.
[b] All calculated IR wavenumbers were scaled with 0.9780.
c PED (Potential Energy Distribution) values lower than10% were not included.
d Letters in parentheses stand for the rings,i.e. (A) for ringA.

*3.2.1.3. C=O stretching modes.* Carbonyl stretching (νC = O) vibration appeared as an intense band in the range of 1600–1800 $cm^{-1}$ [72]. In our previous work [37], carbonyl stretching for the similar benzothiazole compound was reported at 1653 $cm^{-1}$ (IR), 1655 $cm^{-1}$ (Raman) and calculated at 1677 $cm^{-1}$. In this work, carbonyl band ($\nu C_{17} = O_{18}$) for BSN-009 was observed at 1655 $cm^{-1}$ in IR and 1658 $cm^{-1}$ in Raman (Table 5), while carbonyl band ($\nu C_{17} = O_{18}$) for BSN-011 was only observed at 1654 $cm^{-1}$ in IR (Table 6). The corresponding carbonyl bands were calculated at 1675 $cm^{-1}$ for BSN-009 and 1671 $cm^{-1}$ for BSN-011, respectively. Stretching mode belonging to $C_{17}$=$O_{18}$ was observed in Raman spectrum at 1658 $cm^{-1}$ for BSN-009, whereas no band appeared for BSN-011.

**Table 6**
Vibrational wavenumbers and assignments for BSN-011.

| No. | Raman | | Infrared | | | PED (%)[c,d] |
|---|---|---|---|---|---|---|
| | Exp.[a] | Calc.[a] | Exp. | Calc. | | |
| | | | | Unscld.[a] | Scld.[b] | |
| 1 | – | 3349 | 3347 | 3651 | 3571 | νNH(100) $N_9$–$H_{29}$ (B) |
| 2 | – | 3304 | 3303 | 3621 | 3541 | νNH(100) $N_{16}$–$H_{34}$ |
| 3 | – | 3169 | 3178 | 3242 | 3171 | νCH(99) $C_{12}$–$H_{31}$ (C) |
| 4 | – | – | – | 3223 | 3152 | νCH(94) $C_{20}$–$H_{35}$,$C_{21}$–$H_{36}$ (D) |
| 5 | – | 3151 | – | 3222 | 3151 | νCH(93) $C_{23}$–$H_{37}$,$C_{24}$–$H_{38}$,$C_{21}$–$H_{36}$ (D) |
| 6 | – | 3133 | – | 3205 | 3134 | νCH(100) $C_{20}$–$H_{35}$,$C_{21}$–$H_{36}$ (D) |
| 7 | – | 3124 | – | 3199 | 3129 | νCH(92) $C_3$–$H_{28}$,$C_4$–$H_{27}$,$C_5$–$H_{26}$,$C_6$–$H_{25}$ (A) |
| 8 | – | 3115 | 3111 | 3188 | 3118 | νCH(95) $C_3$–$H_{28}$,$C_4$–$H_{27}$,$C_5$–$H_{26}$,$C_6$–$H_{25}$ (A) |
| 9 | – | – | – | 3180 | 3110 | νCH(98) $C_3$–$H_{28}$,$C_4$–$H_{27}$,$C_5$–$H_{26}$,$C_6$–$H_{25}$ (A) |
| 10 | – | 3106 | – | 3178 | 3108 | νCH(90) $C_{15}$–$H_{33}$,$C_{14}$–$H_{32}$ (C) |
| 11 | – | – | – | 3174 | 3104 | νCH(98) $C_{24}$–$H_{38}$,$C_{23}$–$H_{37}$ (D) |
| 12 | – | – | – | 3172 | 3102 | νCH(90) $C_3$–$H_{28}$,$C_4$–$H_{27}$,$C_5$–$H_{26}$,$C_6$–$H_{25}$ (A) |
| 13 | – | 3097 | – | 3164 | 3094 | νCH(99) $C_{11}$–$H_{30}$ (C) |
| 14 | – | 3079 | 3065 | 3149 | 3080 | νCH(90) $C_{14}$–$H_{32}$,$C_{15}$–$H_{33}$ (C) |
| 15 | – | 1675 | 1654 | 1709 | 1671 | νCO(79) $C_{17}$=$O_{18}$ |
| 16 | – | 1603 | 1599 | 1634 | 1598 | νCC(46) $C_{22}$–$C_{23}$,$C_{19}$–$C_{20}$,$C_{20}$–$C_{21}$,$C_{23}$–$C_{24}$ (D) |
| 17 | 1592 | 1594 | 1599 | 1632 | 1596 | νCC(44) $C_{19}$–$C_{24}$,$C_{21}$–$C_{22}$ (D) |
| 18 | 1592 | – | 1589 | 1628 | 1592 | νCC(45) $C_2$–$C_3$,$C_5$–$C_6$,$C_4$–$C_5$,$C_3$–$C_4$ (A) +δHNC(11) $H_{29}$–$N_9$–$C_8$ (B) |
| 19 | – | 1585 | 1589 | 1619 | 1583 | νCC(51) $C_1$–$C_2$, $C_4$–$C_5$,$C_{14}$–$C_{15}$,$C_{11}$–$C_{12}$ (A,C) |
| 20 | – | 1576 | 1589 | 1616 | 1580 | νCC(55) $C_1$–$C_6$, $C_3$–$C_4$,$C_{14}$–$C_{15}$,$C_{11}$–$C_{12}$ (A,C) |
| 21 | – | 1549 | 1557 | 1585 | 1550 | δHNC(44) $H_{34}$–$N_{16}$–$C_{13}$ +νCC(11) $C_{13}$–$C_{14}$ (C) |
| 22 | – | 1531 | 1535 | 1567 | 1533 | νNO(75) $N_{39}$=$O_{40}$, $N_{39}$=$O_{41}$ +δCC(15) $C_{21}$–$C_{22}$,$C_{23}$–$C_{22}$ (D) |
| 23 | – | 1522 | 1520 | 1556 | 1522 | νCC(25) $C_8$–$C_{10}$ +νNC(11) $N_9$–$C_8$ (B) +δHNC(10) $H_{29}$–$N_9$–$C_8$ (B) |
| 24 | – | 1486 | 1488 | 1521 | 1488 | δHCC(27) $H_{38}$–$C_{24}$–$C_{19}$,$H_{35}$–$C_{20}$–$C_{19}$ (D) +νCC(23) $C_{19}$–$C_{20}$,$C_{19}$–$C_{24}$ (D) |
| 25 | – | 1477 | 1478 | 1511 | 1478 | νHCC(48) $H_{26}$–$C_5$–$C_4$,$H_{33}$–$C_{15}$–$C_{10}$,$H_{36}$–$C_{21}$–$C_{20}$ (A,C,D) +δHNC(13) $H_{29}$–$N_9$–$C_2$ |
| 26 | – | – | 1478 | 1508 | 1475 | δHCC(42) $H_{26}$–$C_5$–$C_4$,$H_{31}$–$C_{12}$–$C_{13}$,$H_{38}$–$C_{24}$–$C_{23}$ (A,C,D) +δHNC(23) $H_{34}$–$N_{16}$–$C_{13}$ |
| 27 | – | 1468 | 1457 | 1495 | 1462 | δHCC(42) $H_{25}$–$C_6$–$C_5$,$H_{26}$–$C_5$–$C_4$ (A) +δCCC(11) $C_2$–$C_1$–$C_6$ (A) +νNC(11) $N_9$–$C_2$ |
| 28 | – | 1432 | 1435 | 1468 | 1436 | δHCC(36) $H_{26}$–$C_5$–$C_4$,$H_{27}$–$C_4$–$C_5$,$H_{30}$–$C_{11}$–$C_{12}$ (A,C) +δHNC(30) $H_{29}$–$N_9$–$C_2$,$H_{29}$–$N_9$–$C_8$ (B) |
| 29 | – | 1423 | – | 1452 | 1420 | νCC(45) $C_{11}$–$C_{12}$,$C_{14}$–$C_{15}$ (C) +δHCC(24) $H_{32}$–$C_{14}$–$C_{15}$,$H_{33}$–$C_{15}$–$C_{14}$,$H_{30}$–$C_{11}$–$C_{12}$ (C) |
| 30 | – | 1396 | 1408 | 1431 | 1400 | νCC(43) $C_{23}$–$C_{24}$,$C_{20}$–$C_{21}$ (D) +δHCC(24) $H_{38}$–$C_{24}$–$C_{23}$,$H_{35}$–$C_{20}$–$C_{21}$ (D) |
| 31 | – | 1360 | – | 1394 | 1363 | δHNC(18) $H_{29}$–$N_9$–$C_2$,$H_{29}$–$C_9$–$C_8$ (B) +δHCC(37) $H_{27}$–$C_4$–$C_5$,$H_{27}$–$C_4$–$C_3$ (A) +νCC(12) $C_8$–$C_{10}$+νCN(10) $C_8$–$N_9$ |
| 32 | – | 1324 | 1347 | 1356 | 1326 | νCC(69) $C_{19}$–$C_{20}$,$C_{19}$–$C_{24}$,$C_{20}$–$C_{21}$,$C_{21}$–$C_{22}$,$C_{23}$–$C_{24}$ (D) |
| 33 | – | 1315 | 1312 | 1348 | 1318 | νNO(54) $N_{39}$=$O_{40}$, $N_{39}$=$O_{41}$ +δCCH(19) $H_{31}$–$C_{12}$–$C_{11}$,$H_{30}$–$C_{11}$–$C_{12}$ (C) |
| 34 | – | 1306 | 1312 | 1338 | 1309 | δHCC (33) $H_{33}$–$C_{15}$–$C_{10}$,$H_{31}$–$C_{12}$–$C_{11}$ (C) +δNCC (14) $N_{16}$–$C_{13}$–$C_{14}$ |
| 35 | – | – | 1312 | 1332 | 1303 | νCC(55) $C_1$–$C_2$,$C_1$–$C_6$,$C_4$–$C_5$ (A) +νCC(20) $C_8$–$C_{10}$ +δHCC(13) $H_{26}$–$C_5$–$C_4$ (A) |

**Table 6** (*continued*)

| No. | Raman | | Infrared | | | |
|---|---|---|---|---|---|---|
| | Exp.[a] | Calc.[a] | Exp. | Calc. | | PED (%)[c,d] |
| | | | | Unscld.[a] | Scld.[b] | |
| 36 | – | 1297 | 1288 | 1325 | 1296 | δHCC(64) $H_{35}$–$C_{20}$–$C_{21}$,$H_{37}$–$C_{23}$ –$C_{24}$,$H_{36}$–$C_{21}$–$C_{20}$, $H_{36}$–$C_{21}$–$C_{22}$, $H_{38}$–$C_{24}$–$C_{23}$ (D) + νCN(10) $C_{22}$ –$N_{39}$ |
| 37 | – | – | 1288 | 1321 | 1292 | νCN(40) $C_{13}$–$N_{16}$ +δHCC (31) $H_{35}$ –$C_{20}$–$C_{21}$,$H_{37}$–$C_{23}$–$C_{24}$ (D) +νCC(10) $C_{10}$–$C_{11}$,$C_{12}$–$C_{13}$ (C) |
| 38 | – | 1261 | 1260 | 1285 | 1257 | νNC(27) $N_9$–$C_2$ (B) +δHCC(20) $H_{25}$ –$C_6$–$C_1$ (A) +δNCC(13) $N_9$–$C_2$ –$C_3$ +δHNC(10) $H_{29}$–$N_9$–$C_2$ (B) |
| 39 | – | 1252 | 1252 | 1279 | 1251 | δHNC(40) $H_{29}$–$N_9$–$C_2$ (B) +δHCC(20) $H_{28}$–$C_3$–$C_2$,$H_{27}$–$C_4$ –$C_5$ (A) +νNC(12) $N_9$–$C_2$ (B) |
| 40 | – | 1243 | 1228 | 1270 | 1242 | νCN(40) $C_{13}$–$N_{16}$ +νCN(16) $C_2$–$N_9$ (B) +δHNC(10) $H_{29}$–$N_9$–$C_2$ (B) +νCC(10) $C_{17}$–$C_{19}$ (C) |
| 41 | – | 1216 | – | 1239 | 1212 | νCC(23) $C_{17}$–$C_{19}$ +νCN(18) $C_{17}$ –$N_{16}$ +δHNC(14) $H_{34}$–$N_{16}$ –$C_{13}$ +δHCC(10) $H_{36}$–$C_{21}$–$C_{20}$,$H_{31}$ –$C_{12}$–$C_{11}$ (D,C) |
| 42 | – | 1198 | 1184 | 1220 | 1193 | δHCC(36) $H_{30}$–$C_{11}$–$C_{10}$,$H_{31}$–$C_{12}$ –$C_{11}$ (B) +νNC(13) $N_9$ –$C_8$ +δHNC(10) $H_{34}$–$N_{16}$–$C_{13}$ |
| 43 | – | 1171 | – | 1202 | 1176 | δHCC(78) $H_{35}$–$C_{20}$–$C_{21}$,$H_{36}$–$C_{21}$ –$C_{20}$,$H_{38}$–$C_{24}$–$C_{23}$,$H_{37}$–$C_{23}$–$C_{24}$ (D) |
| 44 | – | 1162 | 1162 | 1192 | 1166 | δHCC(25) $H_{33}$–$C_{15}$–$C_{14}$,$H_{32}$–$C_{14}$ –$C_{15}$ (C) +δNCC(12) $N_9$–$C_8$–$C_{10}$ |
| 45 | – | 1153 | 1162 | 1182 | 1156 | δHCC(79) $H_{26}$–$C_5$–$C_4$,$H_{27}$–$C_4$ –$C_5$,$H_{25}$–$C_6$–$C_5$ (A) |
| 46 | – | 1126 | – | 1150 | 1125 | δHCC(29) $H_{32}$–$C_{14}$–$C_{15}$, $H_{33}$–$C_{15}$ –$C_{14}$,$H_{31}$–$C_{12}$–$C_{11}$,$H_{30}$–$C_{11}$–$C_{12}$ (B) +δHNC (14) $H_{29}$–$N_9$–$C_8$ (B) |
| 47 | – | 1117 | 1112 | 1146 | 1121 | δHCC(42) $H_{20}$–$C_3$–$C_4$,$H_{27}$–$C_4$ –$C_5$,$H_{26}$–$C_5$–$C_6$ (A) +νSC(13) $C_1$ –$S_7$ +νCC(11) $C_1$–$C_2$ |
| 48 | – | 1108 | 1102 | 1131 | 1106 | δHCC(66) $H_{38}$–$C_{24}$–$C_{23}$,$H_{37}$–$C_{23}$ –$C_{24}$,$H_{36}$–$C_{21}$–$C_{20}$,$H_{35}$–$C_{20}$–$C_{21}$ (D) |
| 49 | – | 1090 | – | 1116 | 1091 | νNC(40) $N_{39}$–$C_{22}$ +νCN(14) $N_{16}$ –$C_{17}$ +δHCC(11) $H_{36}$–$C_{21}$–$C_{22}$ (D) |
| 50 | – | 1081 | 1073 | 1110 | 1086 | δCCC(66) $C_{20}$–$C_{21}$–$C_{22}$,$C_{22}$–$C_{23}$–$C_{24}$ (D) +νNC(11) $N_{39}$–$C_{22}$ +νCN(10) $N_{16}$–$C_{17}$ |
| 51 | – | 1054 | – | 1075 | 1051 | νSC(49) $C_1$–$S_7$ (B) +νCC(11) $C_1$ –$C_2$,$C_1$–$C_6$ (A) |
| 52 | – | 1018 | 1014 | 1042 | 1019 | δCCC(73) $C_3$–$C_4$–$C_5$,$C_4$–$C_5$ –$C_6$ +δHCC(12) $H_{28}$–$C_3$–$C_4$,$H_{24}$–$C_6$ –$C_5$,$H_{26}$–$C_5$–$C_4$ (A) |
| 53 | – | 1000 | 1014 | 1028 | 1005 | δCCC(68) $C_{19}$–$C_{20}$–$C_{21}$,$C_{20}$–$C_{21}$ –$C_{22}$,$C_{22}$–$C_{23}$–$C_{24}$ (D) +δHCC(17) $H_{36}$–$C_{21}$–$C_{20}$,$H_{38}$–$C_{24}$–$C_{23}$ (D) |
| 54 | – | 991 | 991 | 1008 | 986 | δCCC(50) $C_{10}$–$C_{11}$–$C_{12}$,$C_{10}$–$C_{15}$–$C_{14}$ (C) +δHCC(15) $H_{33}$–$C_{15}$–$C_{14}$,$H_{31}$ –$C_{12}$–$C_{11}$ (C) |
| 55 | – | 982 | 991 | 1006 | 984 | γHCCC(87) $H_{35}$–$C_{20}$–$C_{21}$–$C_{22}$,$H_{36}$ –$C_{21}$–$C_{20}$–$C_{19}$ out of H (D) |
| 56 | – | 964 | 969 | 982 | 960 | γHCCC(85) $H_{37}$–$C_{23}$–$C_{22}$–$C_{21}$,$H_{38}$ –$C_{24}$–$C_{23}$–$C_{22}$ out of H (D) |
| 57 | – | 946 | 944 | 970 | 949 | γHCCC(89) $H_{26}$–$C_5$–$C_4$–$C_3$,$H_{27}$–$C_4$ –$C_3$–$C_2$ out of H (A) |
| 58 | – | – | 944 | 970 | 949 | γHCCC(86) $H_{31}$–$C_{12}$–$C_{11}$–$C_{10}$,$H_{30}$ –$C_{11}$–$C_{12}$–$C_{13}$ out of H (C) |
| 59 | – | 937 | 944 | 963 | 942 | νSC(34) $C_8$–$S_7$(B) +δHNC (18) $H_{29}$ –$N_9$–$C_8$ (B) |
| 60 | – | 910 | 900 | 933 | 912 | γHCCC(92) $H_{33}$–$C_{15}$–$C_{10}$–$C_8$,$H_{32}$ –$C_{14}$–$C_{13}$–$C_{12}$ out of H (C) |
| 61 | – | 910 | 900 | 926 | 906 | γHCCC(94) $H_{26}$–$C_5$–$C_4$–$C_3$,$H_{27}$–$C_4$ –$C_5$–$C_6$,$H_{25}$–$C_6$–$C_1$–$S_7$,$H_{28}$–$C_3$–$C_2$ –$N_9$ out of H (A) |
| 62 | – | 883 | – | 906 | 886 | δNCO(49) $N_{16}$–$C_{17}$–$O_{18}$ +δCNC(19) $C_{13}$–$N_{16}$–$C_{17}$ +νCC(11) $C_{17}$ –$C_{19}$ +νNC(11) $N_{16}$–$C_{17}$ |

(*continued on next page*)

**Table 6** (*continued*)

| No. | Raman | | Infrared | | | |
|---|---|---|---|---|---|---|
| | Exp.[a] | Calc.[a] | Exp. | Calc. | | PED (%)[c,d] |
| | | | | Unscld.[a] | Scld.[b] | |
| 63 | 862 | 856 | 866 | 879 | 860 | γHCCC(78) $H_{36}$–$C_{21}$–$C_{20}$–$C_{19}$,$H_{35}$–$C_{20}$–$C_{21}$–$C_{22}$ out of H (D) |
| 64 | – | 847 | 853 | 867 | 848 | δCCC(33) $C_4$–$C_5$–$C_6$ (A) +δCCC (15) $C_{10}$–$C_{11}$–$C_{12}$,$C_{10}$–$C_{15}$–$C_{14}$ (C)+ δONO(13) $O_{40}$–$N_{39}$–$O_{40}$ |
| 65 | – | 838 | 853 | 865 | 846 | δONO(41) $O_{40}$–$N_{39}$–$O_{40}$ +δCNO(11) $C_{22}$–$N_{39}$–$O_{40}$,$C_{22}$–$N_{39}$–$O_{41}$ +νCN(10) $C_{22}$–$N_{39}$ |
| 66 | 839 | 829 | 829 | 847 | 828 | γHCCC(82) $H_{35}$–$C_{20}$–$C_{19}$–$C_{17}$,$H_{36}$–$C_{21}$–$C_{22}$–$C_{39}$,$H_{38}$–$C_{24}$–$C_{19}$–$C_{17}$,$H_{37}$–$C_{23}$–$C_{22}$–$C_{39}$ out of H (D) |
| 67 | 839 | 820 | 829 | 839 | 821 | γHCCC(90) $H_{28}$–$C_3$–$C_2$–$C_1$,$H_{25}$–$C_6$–$C_1$–$C_2$, $H_{26}$–$C_5$–$C_6$–$C_1$,$H_{27}$–$C_4$–$C_3$–$C_2$ out of H (A) |
| 68 | – | 811 | – | 827 | 809 | νCN(39) $C_{13}$–$N_{16}$ +νCC(20) $C_{12}$–$C_{13}$,$C_{13}$–$C_{14}$ (C) +γHCCC(10) $H_{38}$–$C_{24}$–$C_{19}$–$C_{20}$,$H_{37}$–$C_{23}$–$C_{22}$–$C_{21}$ out of H (D) |
| 69 | – | 775 | 777 | 795 | 778 | γHCCC(86) $H_{30}$–$C_{11}$–$C_{10}$–$C_8$,$H_{31}$–$C_{12}$–$C_{13}$–$N_{16}$,$H_{33}$–$C_{15}$–$C_{10}$–$C_8$,$H_{32}$–$C_{14}$–$C_{13}$–$N_{16}$ out of H (C) |
| 70 | – | 766 | 765 | 787 | 770 | γHCCC(86) $H_{30}$–$C_{11}$–$C_{10}$–$C_8$,$H_{31}$–$C_{12}$–$C_{13}$–$N_{16}$,$H_{33}$–$C_{15}$–$C_{10}$–$C_8$,$H_{32}$–$C_{14}$–$C_{13}$–$N_{16}$ out of H (C) |
| 71 | – | 748 | – | 763 | 746 | γONCC(79) $O_{18}$–$N_{16}$–$C_{17}$–$C_{19}$ +τHCCC(18) $C_{24}$–$C_{20}$–$C_{19}$–$C_{17}$ (D) |
| 72 | – | 730 | 732 | 746 | 730 | γHCCC(86) $H_{25}$–$C_6$–$C_5$–$C_4$,$H_{27}$–$C_4$–$C_3$–$C_2$,$H_{28}$–$C_3$–$C_2$–$C_1$,$H_{26}$–$C_5$–$C_6$–$C_1$ out of H (A) |
| 73 | – | 712 | 713 | 728 | 712 | δCNO(17) $C_{22}$–$N_{39}$–$O_{40}$,$C_{22}$–$N_{39}$–$O_{41}$ + δCCC(15) $C_{19}$–$C_{20}$–$C_{21}$,$C_{21}$–$C_{22}$–$C_{23}$,$C_{19}$–$C_{24}$–$C_{23}$ (D) +δCCN(14) $C_{21}$–$C_{22}$–$N_{39}$ +νCC(13) $C_{21}$–$C_{22}$ (D) |
| 74 | – | 703 | 697 | 713 | 697 | τCCCC(44) $C_{10}$–$C_{11}$–$C_{12}$–$C_{13}$,$C_{10}$–$C_{15}$–$C_{14}$–$C_{13}$,$C_3$–$C_2$–$C_1$–$C_6$ (C,A) +γONCC(19) $O_{18}$–$N_{16}$–$C_{17}$–$C_{19}$ |
| 75 | – | – | 697 | 711 | 695 | νSC(27) $C_1$–$S_7$ +δCCC(23) $C_2$–$C_1$–$C_6$,$C_3$–$C_4$–$C_5$ (A) |
| 76 | – | 694 | 697 | 710 | 694 | γONOC(60) $O_{40}$–$N_{39}$–$O_{41}$–$C_{22}$ +γHCCC(29) $H_{37}$–$C_{23}$–$C_{22}$–$C_{21}$,$H_{36}$–$C_{21}$–$C_{22}$–$C_{23}$ out of H (D) |
| 77 | – | 685 | – | 705 | 689 | τCCCC(78) $C_1$–$C_2$–$C_3$–$C_4$,$C_5$–$C_6$–$C_1$–$C_2$,$C_{10}$–$C_{11}$–$C_{12}$–$C_{13}$,$C_{10}$–$C_{15}$–$C_{14}$–$C_{13}$ (A,C) |
| 78 | – | 667 | 678 | 685 | 670 | νSC(26) $S_7$–$C_8$ +δNCC(17) $N_9$–$C_8$–$C_{10}$ |
| 79 | – | 658 | – | 675 | 660 | γONCC(59) $O_{18}$–$N_{16}$–$C_{17}$–$C_{19}$ +τCCCC(30) $C_{17}$–$C_{19}$–$C_{20}$–$C_{21}$,$C_{17}$–$C_{19}$–$C_{24}$–$C_{23}$ (D) |
| 80 | – | 631 | 644 | 647 | 633 | δCCN(51) $C_{12}$–$C_{13}$–$N_{16}$,$C_3$–$C_2$–$N_9$ +δCCC(17) $C_4$–$C_5$–$C_6$,$C_{11}$–$C_{12}$–$C_{13}$ (A,C) +δCNC(11) $C_2$–$N_9$–$C_8$ |
| 81 | – | – | 620 | 643 | 629 | δCCC(72) $C_{19}$–$C_{24}$–$C_{23}$,$C_{19}$–$C_{20}$–$C_{21}$ (D) |
| 82 | – | 622 | 620 | 640 | 626 | δCCC(71) $C_{11}$–$C_{12}$–$C_{13}$,$C_{10}$–$C_{15}$–$C_{14}$ (C) |
| 83 | – | 559 | – | 575 | 562 | γHNCC(66) $H_{34}$–$N_{16}$–$C_{13}$–$C_{12}$ out of N |
| 84 | – | 550 | 552 | 567 | 555 | γHNCC(37) $H_{34}$–$N_{16}$–$C_{13}$–$C_{12}$ out of N |
| 85 | – | 532 | 534 | 542 | 530 | τCCCC(79) $C_3$–$C_4$–$C_5$–$C_6$,$C_1$–$C_6$–$C_5$–$C_4$ (A) +γCCCN(10) $C_6$–$C_1$–$C_2$–$N_9$ (B) |
| 86 | – | 523 | 534 | 541 | 529 | γHNCC(32) $H_{34}$–$N_{16}$–$C_{13}$–$C_{12}$ out of N +δCCN(51) $C_{23}$–$C_{22}$–$N_{39}$ |
| 87 | – | 514 | 503 | 517 | 506 | δCNO(41) $C_{22}$–$N_{39}$–$O_{40}$,$C_{22}$–$N_{39}$–$O_{41}$ +δCCO(14) $O_{18}$–$C_{17}$–$C_{19}$ +δCCN(10) $C_{21}$–$C_{22}$–$N_{39}$ |

**Table 6** (*continued*)

| No. | Raman | | Infrared | | | PED (%)[c,d] |
|---|---|---|---|---|---|---|
| | Exp.[a] | Calc.[a] | Exp. | Calc. | | |
| | | | | Unscld.[a] | Scld.[b] | |
| 88 | – | 496 | – | 505 | 494 | γHCCC(75) $H_{30}$–$C_{11}$–$C_{10}$–$C_{15}$ out of H (C) +τCCCS(10) $S_7$–$C_8$–$C_{10}$–$C_{15}$ (C) |
| 89 | – | 487 | 483 | 498 | 487 | δCSC(57) $C_1$–$S_7$–$C_8$ (B) +δSCN(12) $S_7$–$C_8$–$N_9$ (B) |
| 90 | – | 451 | 459 | 461 | 451 | γHCCC(20) $H_{36}$–$C_{21}$–$C_{22}$–$C_{23}$,$H_{38}$–$C_{24}$–$C_{23}$–$C_{22}$ out of H (D) |
| 91 | – | 424 | 422 | 431 | 422 | δSCC(18) $S_7C_8C_{10}$ +δCNC(12) $C_{13}$–$N_{16}$–$C_{17}$ +δNCC(10) $N_9$–$C_8$–$C_{10}$ |
| 92 | 411 | 415 | 411 | 425 | 416 | τCCCC(44) $C_3$–$C_2$–$C_1$–$C_6$,$C_4$–$C_3$–$C_2$–$C_1$ (A) |
| 93 | 411 | 406 | 411 | 421 | 412 | τCCCC(92) $C_{22}$–$C_{21}$–$C_{20}$–$C_{19}$,$C_{22}$–$C_{23}$–$C_{24}$–$C_{19}$ (D) |
| 94 | 411 | – | 411 | 417 | 408 | τCCCC(32) $C_{10}$–$C_{11}$–$C_{12}$–$C_{18}$,$C_{10}$–$C_{15}$–$C_{14}$–$C_{13}$ (C) |
| 95 | – | 397 | – | 404 | 395 | δCCC(29) $C_{17}$–$C_{19}$–$C_{24}$ +δNCC(13) $N_{16}$–$C_{17}$–$C_{19}$ +δCNO(12) $C_{22}$–$N_{39}$–$O_{40}$ +δCCS(10) $C_6$–$C_1$–$S_7$ |
| 96 | – | 379 | – | 389 | 380 | γSCNC(52) $S_7$–$C_{10}$–$N_9$–$C_8$ +τCCNC(11) $C_{12}$–$C_{13}$–$N_{16}$–$C_{17}$ |
| 97 | – | 361 | – | 370 | 362 | δCCN(33) $C_{14}$–$C_{13}$–$N_{16}$ +δNCO(33) $N_{16}$–$C_{17}$–$O_{18}$ |
| 98 | – | 316 | – | 319 | 312 | δCNC(37) $C_{13}$–$N_{16}$–$C_{17}$ +δCCC(14) $C_{17}$–$C_{19}$–$C_{20}$ +δNCS(12) $N_9$–$C_8$–$S_7$ |
| 99 | – | 298 | – | 305 | 298 | τNCCC(50) $N_9$–$C_8$–$C_{10}$–$C_{15}$ |
| 100 | – | 280 | – | 289 | 283 | τCNCC(10) $C_{13}$–$N_{16}$–$C_{17}$–$C_{19}$ +δCCN(10) $C_{23}$–$C_{22}$–$N_{39}$ +δCCC(10) $C_{17}$–$C_{19}$–$C_{20}$ |
| 101 | – | 271 | – | 275 | 269 | τHNCC(48) $H_{29}$–$N_9$–$C_2$–$C_1$ |
| 102 | – | 262 | – | 269 | 263 | τHNCC(21) $H_{29}$–$N_9$–$C_8$–$C_{10}$ |
| 103 | – | 244 | – | 249 | 244 | τCCCC(35) $C_1$–$C_6$–$C_5$–$C_4$ +τHNCC(16) $H_{29}$–$N_9$–$C_8$–$C_{10}$ +τCNCC(11) $C_{13}$–$N_{16}$–$C_{17}$–$C_{19}$ |
| 104 | – | 226 | – | 234 | 229 | τCCCN(56) $C_4$–$C_3$–$C_2$–$N_9$ +γSCNC(13) $S_7$–$C_{10}$–$N_9$–$C_8$ |
| 105 | – | 181 | – | 189 | 185 | δCCN(55) $C_{21}$–$C_{22}$–$N_{39}$ +δCCC(15) $C_{17}$–$C_{19}$–$N_{20}$ +δCCN(13) $C_{14}$–$C_{13}$–$N_{16}$ +δNCC(10) $N_9$–$C_8$–$C_{10}$ |
| 106 | – | 172 | – | 176 | 172 | τSCCH(67) $S_7$–$C_1$–$C_6$–$H_{25}$ +τNCCH(11) $N_9$–$C_2$–$C_3$–$H_{28}$ |
| 107 | – | 136 | – | 136 | 133 | τCCNC(34) $C_{14}$–$C_{13}$–$N_{16}$–$C_{17}$ |
| 108 | – | 127 | – | 133 | 130 | δCNC(11) $C_{13}$–$N_{16}$–$C_{17}$ +τCCNC(10) $C_{14}$–$C_{13}$–$N_{16}$–$C_{17}$ |
| 109 | – | 91 | – | 92 | 90 | τCCCN(43) $N_{16}$–$C_{17}$–$C_{19}$–$C_{24}$ +τCNCC(26) $C_2$–$N_9$–$C_8$–$C_{10}$ |
| 110 | – | 82 | – | 81 | 79 | τOCCC(49) $O_{18}$–$C_{17}$–$C_{19}$–$C_{24}$ +γCCNC(11) $C_{12}$–$C_{13}$–$N_{16}$–$C_{17}$ |
| 111 | – | 64 | – | 71 | 69 | γCNCC(13) $C_{13}$–$N_{16}$–$C_{17}$–$C_{19}$+δCNC(13) $C_{13}$–$N_{16}$–$C_{17}$ |
| 112 | – | 55 | – | 56 | 55 | τCCNO(78) $C_{21}$–$C_{22}$–$N_{39}$–$O_{40}$,$C_{21}$–$C_{22}$–$N_{39}$–$O_{41}$ |
| 113 | – | 46 | – | 41 | 40 | τCNCC(53) $C_{12}$–$C_{13}$–$N_{16}$–$C_{17}$,$C_{14}$–$C_{13}$–$N_{16}$–$C_{17}$ |
| 114 | – | 37 | – | 38 | 37 | τCNCC(34) $C_2$–$N_9$–$C_8$–$C_{10}$,$C_{13}$–$N_{16}$–$C_{17}$–$C_{19}$ +δCNC(12) $C_2$–$N_9$–$C_8$ |
| 115 | – | 28 | – | 30 | 29 | δCNC(22) $C_{13}$–$N_{16}$–$C_{17}$ +τCNCC(15) $C_2$–$N_9$–$C_8$–$C_{10}$ +τCCNC(13) $C_{14}$–$C_{13}$–$N_{16}$–$C_{17}$ |
| 116 | – | 19 | – | 21 | 21 | τCCNC(61) $C_{14}$–$C_{13}$–$N_{16}$–$C_{17}$ +τCNCC(16) $C_2$–$N_9$–$C_8$–$C_{10}$ |
| 117 | – | 10 | – | 12 | 12 | τCNCC(34) $C_{13}$–$N_{16}$–$C_{17}$–$C_{19}$ +τCCNC(21) $C_2$–$N_9$–$C_8$–$C_{10}$ +τCCCC(10) $C_{17}$–$C_{19}$–$C_{24}$–$C_{23}$ |

[a] Exp.:Experimental, Calc.:Calculated, Unscld:Unscaled, Scld.:Scaled.
[b] All calculated IR wavenumbers were scaled with 0.9780.
[c] PED (Potential Energy Distribution) values lower than 10% were not included.
[d] Letters in parentheses stand for the rings, i.e. (A) for ring A.

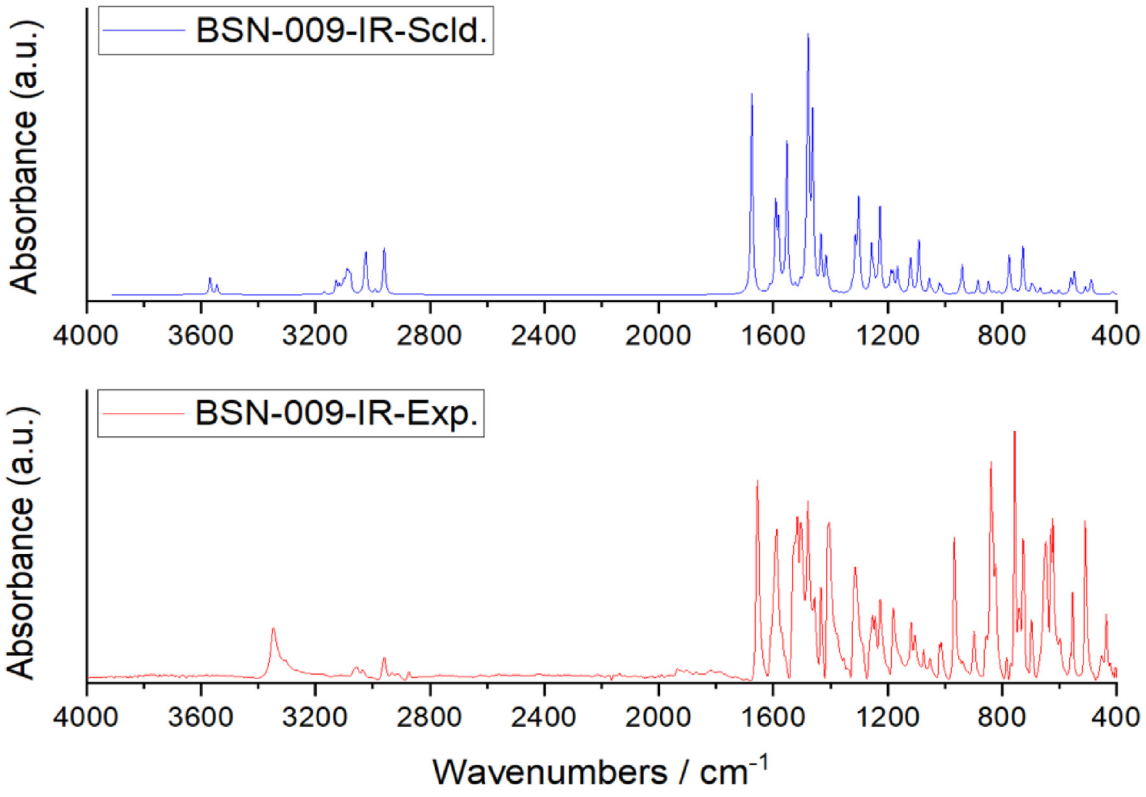


**Fig. 7.** The experimental and calculated IR spectra of BSN-009 (1).

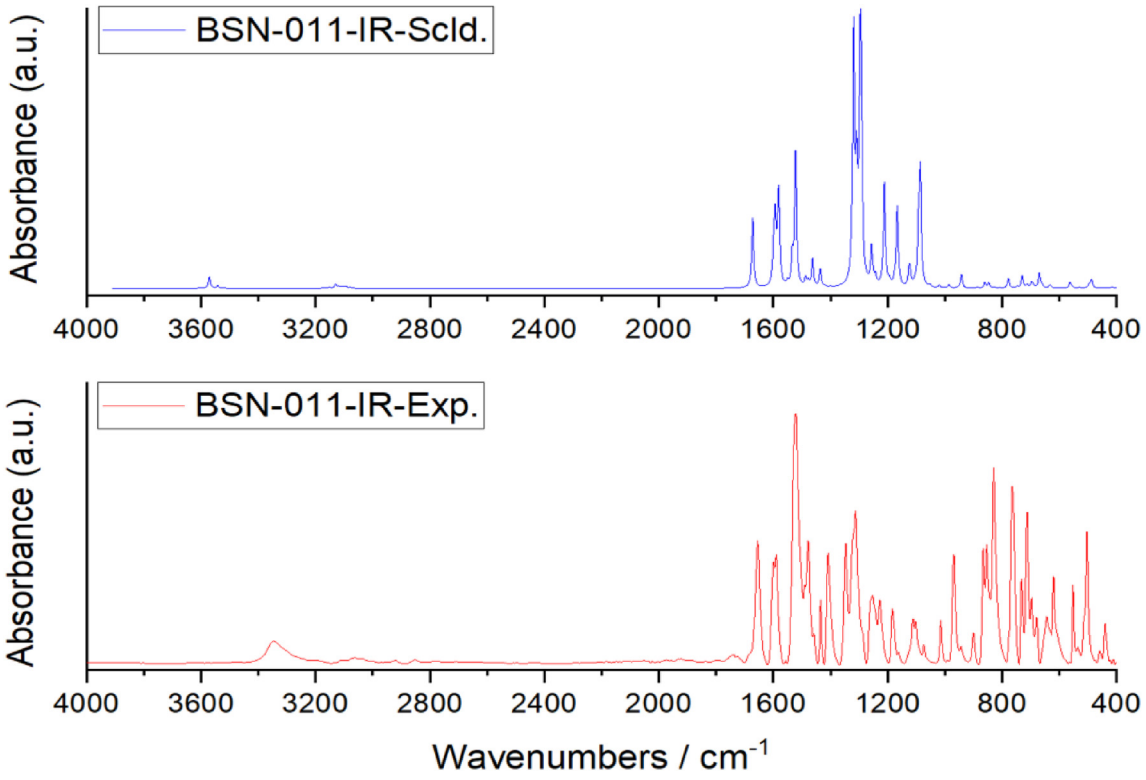


**Fig. 8.** The experimental and calculated IR spectra of BSN-011 (1).

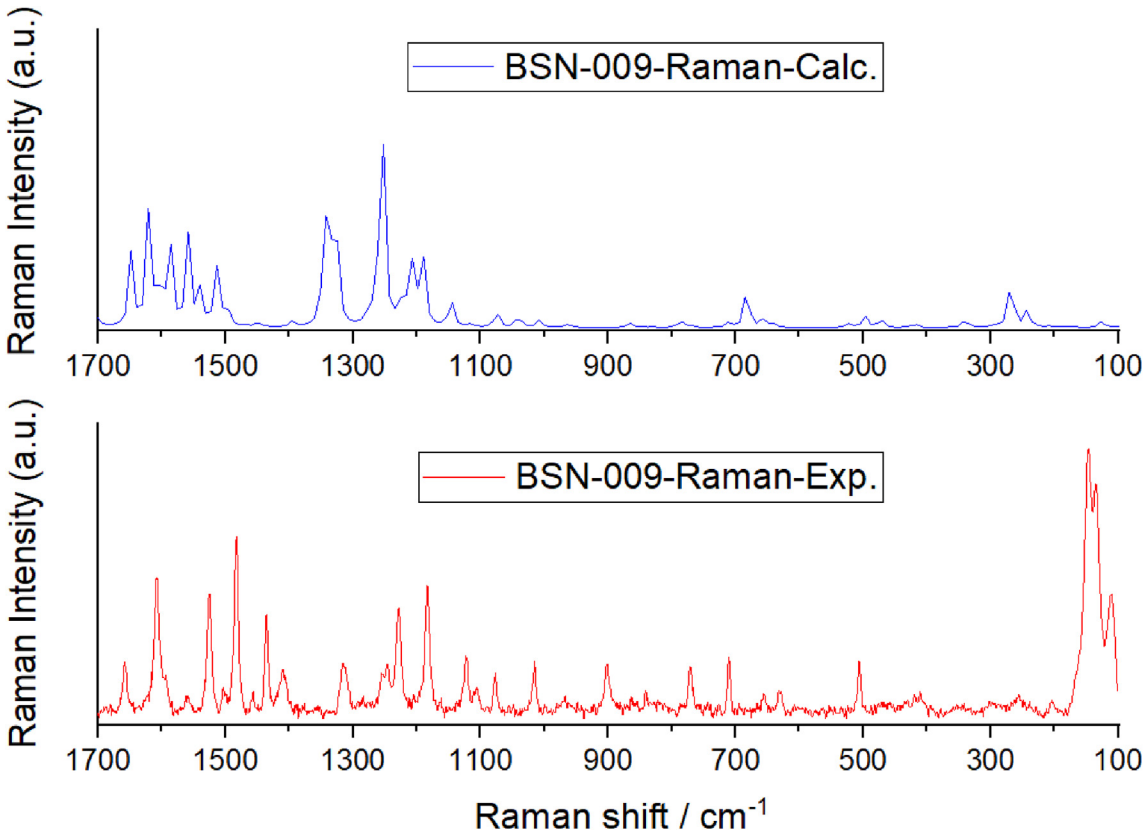


**Fig. 9.** The experimental and calculated Raman spectra of BSN-009 (1).

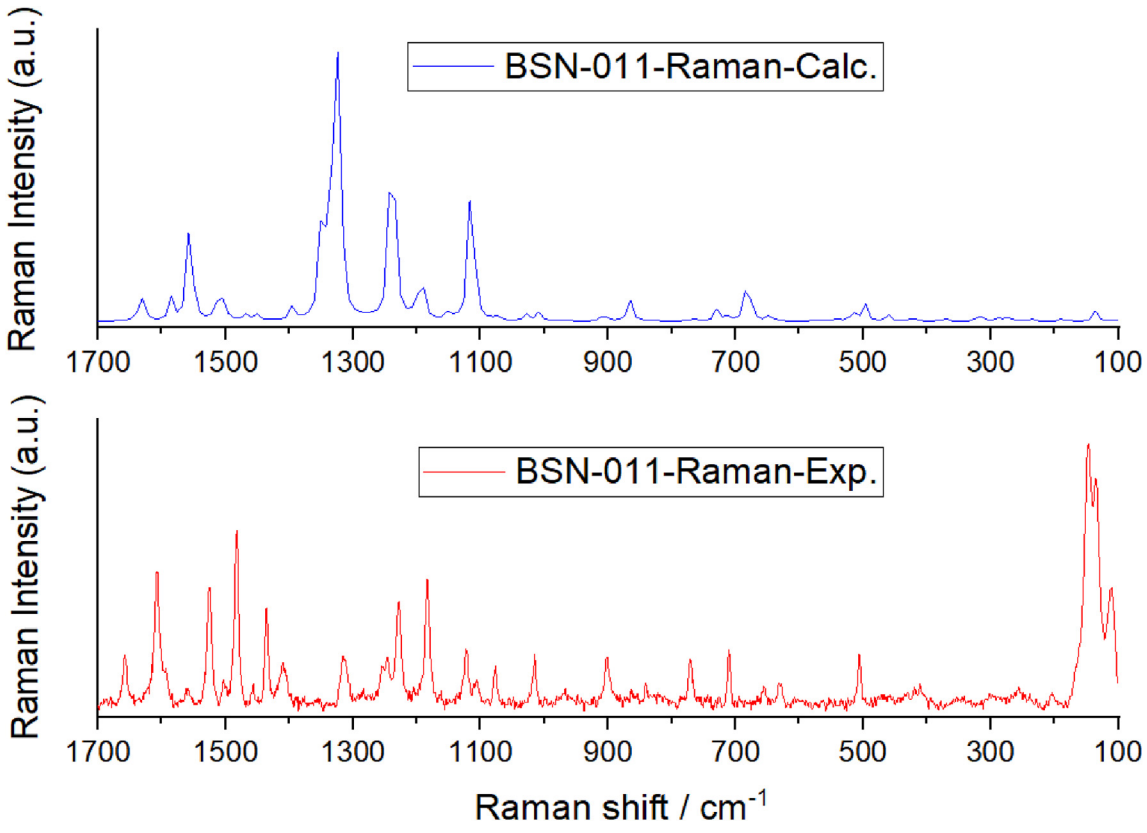


**Fig. 10.** The experimental and calculated Raman spectra of BSN-011 (1).

*3.2.1.4. N=O stretching modes.* The stretching vibrations of nitro (-$NO_2$) group (νN = O) were reported within the range of 1580-1345 $cm^{-1}$ in substituted nitrobenzenes [72]. The bands calculated at 1533 (observed at 1535 $cm^{-1}$) and 1318 $cm^{-1}$ (observed at 1312 $cm^{-1}$) in IR spectrum of BSN-011 were attributed to the N=O stretching modes (Table 6). Since BSN-011 does not have any nitro moiety, no IR mode was observed. In addition, Raman spectrum of BSN-011 did not exhibit any Raman active nitro group stretching mode.

*3.2.1.5. C–N and C=N stretching modes.* The C–N stretching vibrations were calculated in the range of 1524-809 $cm^{-1}$ for both compounds with decreasing wavenumber order; $\nu C_8$-$N_9$>$\nu C_2$-$N_9$>$\nu C_{13}$-$N_{16}$>$\nu C_{17}$-$N_{16}$ (coupled with CC stretching, CCH and CNH in-plane bending and the other modes). While the most dominant C–N stretching mode ($C_{17}$–$N_{16}$) was observed at 1226 $cm^{-1}$ in IR spectrum (1228 $cm^{-1}$ in experimental Raman) of BSN-009 (PED: 31%) and these modes were coupled with some CCH in plane bending vibrations (see *3.2.2.* section) even by contribution values between 10 and 16% (mode numbers 27, 33, 39, 47 and 50 in Table 5), they were also added as contribution to this stretching mode and presented here. IR active C=N stretching modes for BSN-009 were observed at 1515, 1456, 1353, 1244, 1226 and 1180 $cm^{-1}$. In Raman spectrum of BSN-009, only Raman active modes for this stretching mode were at 1525, 1249 and 1183 $cm^{-1}$. In addition, from the calculated Raman spectra for BSN-009, we could determine these bands at 1513 and 1189 $cm^{-1}$. In contrast, for BSN-011, this stretching mode was not active in its Raman spectrum. Moreover, only the most dominant N–C stretching mode represents the bond which links the ring C to ring D ($N_{16}$–$C_{17}$) was not observed in any experimental vibrational spectra, but calculated at 1090 and 1091 $cm^{-1}$ (PED: 53% and number of the mode is 59 in Table 5) in theoretical Raman and IR spectra for BSN-009. This mode was also coupled with CC stretching observed at 1226 $cm^{-1}$ (experimental IR, mode number is 50 with PED of 13%) and δNCO (in-plane NCO bending) calculated at 884 $cm^{-1}$ (IR, mode number is 74 with PED of 10%). As for BSN-011, stretching mode ($N_{16}$–$C_{17}$) was coupled with various stretching ($C_{17}$–$C_{19}$ calculated at 1212 $cm^{-1}$ (IR) and $N_{39}$–$C_{22}$ calculated at 1091 $cm^{-1}$ (IR) with corresponding mode numbers 41 and 49, respectively) and bending modes ($C_{20}C_{21}C_{22}$ observed at 1073 $cm^{-1}$ in IR spectrum (mode number 50). C=N ($C_8N_9$) stretching mode for BSN-011 was observed at 1520 $cm^{-1}$ in IR spectrum (not Raman active, ca. Ra at 1522 $cm^{-1}$). Arjunan et al. [50] observed the C=N stretching mode at 1513 $cm^{-1}$ (IR), 1516 $cm^{-1}$ (Raman) and calculated at 1523 $cm^{-1}$ for 2-benzothiazole acetonitrile. In this study, corresponding band is observed at 1515 $cm^{-1}$ (IR), 1525 $cm^{-1}$ (Raman) and calculated at 1524 $cm^{-1}$ for BSN-009; at 1520 $cm^{-1}$ (IR), (no Raman band) and calculated at 1524 $cm^{-1}$ for BSN-011. These results are in consistent with our observations.

*3.2.1.6. C–S stretching modes.* The bands observed at 1117, 1053, 937 and 698 $cm^{-1}$ in experimental IR for BSN-009 and 1112, 944, 697 and 678 $cm^{-1}$ in IR for BSN-011 were assigned to C–S stretching vibrations. On the other hand, one of these modes was coupled with a CCH in-plane bending mode (PED: 41% with mode number 57). These vibrational modes were calculated at 1119, 1051, 939, 694 and 667 $cm^{-1}$ for BSN-009 and 1121, 1051, 942, 695 and 670 $cm^{-1}$ for BSN-011. None of these stretching modes were active in experimental Raman spectra, but corresponding modes were calculated at 937, 694 for BSN-009 and 1117, 1054, 944 and 678 $cm^{-1}$ for BSN-011.

*3.2.2. Bending (in-plane and out-of-plane) and torsional modes*

*3.2.2.1. Aromatic CCH in-plane bending modes.* CCH in plane bending vibrations (δCCH) for BSN-009 and BSN-011 within A, C and D ring were observed in 1503-1053 $cm^{-1}$ and 1488-1102 $cm^{-1}$ regions in IR spectra, respectively. For BSN-009, corresponding calculated wavenumbers for these related bending modes in theoretical Raman spectra were at 1504 (observed at 1498 $cm^{-1}$ in experimental (exp.) Raman (Ra) spectrum), 1477, 1378, 1342, 1315 (1314 $cm^{-1}$, exp. Ra), 1306, 1243 (observed at 1241 $cm^{-1}$ in exp. Ra), 1189 (1183 $cm^{-1}$ exp. Ra.), 1180, 1126 (observed at 1123 $cm^{-1}$ exp. Ra.) and 1054 $cm^{-1}$. In addition, CCH in plane bending vibrations in theoretical Raman spectrum for BSN-011 were also calculated at 1486, 1432, 1306, 1297, 1198, 1162, 1153, 1126, 1117 and 1108 $cm^{-1}$. However, no experimental Raman active bands were observed for BSN-011.

*3.2.2.2. Aliphatic HCH and CCH in-plane bending modes.* The ethyl group HCH modes of BSN-009 appeared in the region of 1479-1053 $cm^{-1}$ in IR spectrum and were calculated in the range of 1475-1044 $cm^{-1}$. The wavenumbers observed at 1377-1053 $cm^{-1}$ were assigned to CCH in-plane bending modes and they were calculated between 1379 and 1044 $cm^{-1}$. The only Raman active HCH bending mode was observed at 1454 $cm^{-1}$ for BSN-009. Since there is no HCH angle for BSN-011, not any vibrational mode was observed for this compound.

*3.2.2.3. CCC in-plane bending modes of the rings.* The bands appeared at 1018, 1012, 987, 855, 630, 623 and 597 $cm^{-1}$ in IR and 1015, 985, 841 and 629 $cm^{-1}$ in Raman spectrum for BSN-009 and the bands at 1073, 1014, 991, 853 and 620 $cm^{-1}$ for BSN-011 were attributed to CCC in plane bending vibrations (δCCC). No Raman vibrational mode was observed for BSN-011.

*3.2.2.4. HNC in-plane bending modes.* The HNC in plane bending vibrations (δHNC) were calculated in 1591-1123 $cm^{-1}$ region and were observed experimentally in the region of 1588-1130 $cm^{-1}$. These modes were experimentally observed at 1558, 1479, 1353 and 1244 $cm^{-1}$ for IR and only observed at 1483 and 1249 $cm^{-1}$ for Raman, respectively.

*3.2.2.5. CSC and SCN in-plane bending modes.* The in-plane bending vibration of CSC for BSN-009 was observed at 469 $cm^{-1}$ (IR), 468 $cm^{-1}$ (Raman) and calculated at 486 $cm^{-1}$ (52% contribution of PED) and the same mode for BSN-011 was observed at 483 $cm^{-1}$ (IR) and calculated at 487 $cm^{-1}$ (PED: 57%). These modes are coupled with SCN in plane bending modes.

*3.2.2.6. Out-of-plane bending and torsional modes.* Since the rest of the compounds have the same geometry (Fig. 1), the most important out-of-plane bending (γ) and torsional modes (τ) are the ones which related to functional groups attached to two ends of both compounds ($C_2H_5$ for BSN-009 and $NO_2$ for BSN-011). These modes are related to the $C_{22}$, $C_{39}$, $H_{40}$, $H_{41}$, $C_{42}$, $H_{43}$, $H_{44}$ and $H_{45}$ atoms for BSN-011 and $C_{22}$, $N_{39}$, $O_{40}$ and $O_{41}$ atoms for BSN-011, respectively. γHCCC out-of-bending modes were observed in IR spectrum for BSN-009 at 947, 897 (901 $cm^{-1}$, calculated Raman) and 822 $cm^{-1}$ (observed at 823 $cm^{-1}$ in Raman spectrum) for the ring A (mode numbers: 70 and 73). In IR and Raman spectra (hereafter, Ra) of BSN-009, these modes were observed at 966 $cm^{-1}$ (967 $cm^{-1}$, Ra), 947 $cm^{-1}$, 855 $cm^{-1}$ (841 $cm^{-1}$, Ra) and 839 $cm^{-1}$ for ring D. The wavenumbers assigned to these same modes were observed at 947 $cm^{-1}$, 897 $cm^{-1}$ (902 $cm^{-1}$, Ra), 770 $cm^{-1}$ (771 $cm^{-1}$) and 481 $cm^{-1}$ for ring C in BSN-009. For BSN-011, γONOC ($O_{40}N_{39}O_{41}C_{22}$) mode was observed at 697 in experimental IR spectrum (calculated at 694 with PED value of 60%) and calculated at 694 in Raman spectrum.

Torsional modes (τHCCC) that represent the end functional

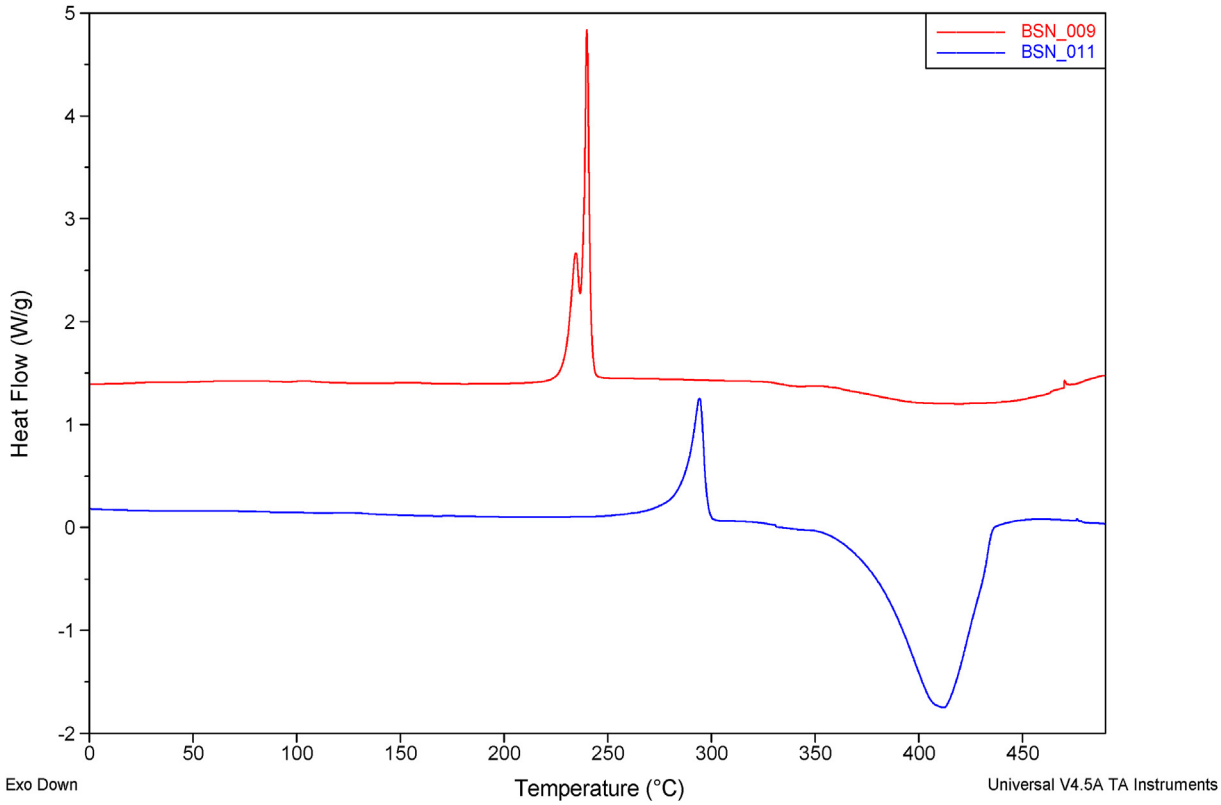


**Fig. 11.** DSC curves for BSN-009 and BSN-011.

group (ring D) of BSN-009 were only calculated at 332 $cm^{-1}$ (334 $cm^{-1}$, calculated Ra), 225 $cm^{-1}$ (226 $cm^{-1}$, calculated Ra) and 203 $cm^{-1}$ (208 $cm^{-1}$, calculated Ra and 203 $cm^{-1}$ observed Ra). As well as BSN-009, only torsional mode (τCCNO) for the $NO_2$ moiety of BSN-011 was only calculated at 55 $cm^{-1}$ (55 $cm^{-1}$, calculated Ra).

### 3.3. DSC studies

DSC was used to get information about the thermal behavior and physicochemical properties of two potential antibacterial agents, BSN-009 and BSN-011. DSC curves of BSN-009 and BSN-011 were shown in Fig. 11. Two sharp endothermic peaks were observed at 234.56 and 239.87 °C corresponding to the melting of BSN-009 with the enthalpy (ΔH) value of 100.3 J/g, whereas only a single endothermic peak was observed at 294.23 °C with the ΔH value of 76.8 J/g for BSN-011. These melting point data were seen to be in consistency with the data which was previously reported to be between 238 and 240 °C for BSN-009 and 296–298 °C for BSN-011 [29]. Furthermore, an intensive exothermic peak appeared at 411.92 °C due to the thermal decomposition of BSN-011, while the thermal decomposition of BSN-009 was observed in the temperature range of 350–500 °C with the peak temperature of 420 °C. The purity of both compounds was also determined by DSC and the degrees of purities for BSN-009 and BSN-011 were found to be 95 and 94 mol%, respectively.

## 4. Discussion

It was previously shown that there is a strong connection between MIC values and antibacterial and antifungal activities of BSN-009 and BSN-011 with certain control drugs and it was revealed that both compounds are good potential compounds against *C. albicans*, but not better as antifungal agents. In contrast to BSN-009 showed better antibacterial activity against both *S. aureus* isolate *(s.a.i.)* (MIC: 6.25 μg/ml) and *Klebsiella pneumoniae (k.p.) RSKK 574* (MIC: 25 μg/ml), BSN-011 (MIC: 12.5 μg/ml for *s.a.* and 50 μg/ml for *k.p.*) showed less antibacterial activity than BSN-009 [27]. On the other hand, our results showed that BSN-011 did not have any violation to Lipinski's rule of five, but BSN-009 violated this rule by the partition coefficient of 5.42 (which should be ≤ 5) (Table 4). Furthermore, bioactivity scores for both compounds given in Table 4 and it was suggested that BSN-009 acts as a GPCR ligand, good nuclear receptor ligand and enzyme inhibitor since a bioactivity score between −0.5 and 0 means it is moderately active. However, even this result indicated that BSN-009 compound can be treated as a potential candidate for bioactive application compared to BSN-011, it still violates Lipinski's rule of five thus, we can eliminate this option. Since BSN-011 does not violate rule of five and still bioactivity scores are between −0.5 and 0, it can be regarded as a potential candidate for bioactive application instead of BSN-009.

By considering the molecular geometry is in the gas phase in our calculations, it must be emphasized that the geometry of these compounds might be in different forms than their solid state. On the other hand, it is also possible to isolate compounds by matrix isolation IR spectroscopic technique in an inert gas environment (helium, xenon, argon etc.) and better evaluate this gas phase computation [36]. In order to confirm this, complementary spectroscopic and structural investigation techniques should be conducted in a systematic way anytime. One of the main advantages of quantum chemistry calculations is that, because of its highly accurate prediction of structure and vibrational wavenumbers, it is a very powerful tool to detect subtle structural and vibrational changes, helped by results of calculated spectra for the investigated compound in gas phase and vacuo. Regarding our quantum chemistry results, we can say that there is a reasonably good

agreement between calculated and experimental vibrational wavenumbers. After conformational analysis performed on molecular structures of BSN-009 and BSN-011, six stable conformers for BSN-009 and four stable conformers for BSN-011 were obtained. Dipole moments of the six conformers of BSN-009 vary from 1.77 D (conformer 1) to 6.19 D (conformer 5), whereas from 7.30 D (conformer 3) to 9.98 D (conformer 2) for the four conformers of BSN-011. The HOMO of both compounds is located around benzothiazole moiety (mostly S atom), phenyl and amide parts, whereas the LUMO around the entire compounds (except ethyl group for BSN-009; mostly nitrobenzene part for BSN-011). According to the plots depict the MEP surfaces of BSN-009 (1) and BSN-011 (1), the electropositive regions are located over the N—H groups while the electronegative regions are located over the oxygen atoms and these regions can be considered as the sites for nucleophilic and electrophilic attacks, respectively.

$C_3$, $S_7$, $C_{13}$, $C_{15}$, $C_{21}$, $C_{23}$, $C_{24}$ and $C_{42}$ atoms for BSN-009 and $C_3$, $S_7$, $C_{13}$, $C_{15}$ and $C_{22}$ atoms for BSN-011 exhibit huge negative charge, which are donor atoms. $C_1$, $C_{10}$, $C_{19}$ and $C_{22}$ atoms for BSN-009 and $C_1$, $C_{10}$ and $C_{19}$ atoms for BSN-011 exhibit huge positive charges which are acceptor atoms. While $C_3$ atom (−0.657) has the highest negative Mulliken atomic charge in BSN-009 compound, this atom has the highest negative value (−0.591) after $C_{22}$ atom (−0.624) where $NO_2$ group is bound in BSN-011 compound. In addition, it is seen that $C_1$ (1.214) atom for BSN-009 and $C_{10}$ (1.051) atom for BSN-011 have higher Mulliken atomic charges than other positive atoms.

By Raman and IR studies we performed in this study, corresponding wavenumbers of the most important portions of these compounds were successfully observed in IR and Raman spectra and theoretically were calculated for the first time. Thus, in near future, our results would shed light on to experimental and modelled spectra of new derivatives and their functions and be helpful in order to better understand their action mechanism as drug candidates as well as their potential bioactive applications. In general, spectroscopically we showed the differences of both compounds and revealed that specific functional groups play different activity which was confirmed by their vibrational spectra and drug likeliness and bioactivity scores.

Since drug polymorphism is related to the different crystallographic structures and polymorphic transitions, any thermal change that occurs during heating by DSC play an important role in understanding crystallographic state and possible polymorphic transitions of the compound under study. Detailed information on interconversion of various polymorphs of candidate drugs is required because the action of the drug depends on its form [47]. In our study, we did not encounter any polymorphic transition neither for BSN-009 nor for BSN-011, but determined their melting points, decomposition and purity features successfully. Additionally, like drug polymorphism, drug purity is of importance since it is not desired to have any impurities in a drug because it will cause unexpected interactions with drug and thus causes improper functions that is not expected. Drug purities were very well discussed previously for 115 drugs [73] by using DSC and a thorough review with a discussion of advantages of this method was also published [74]. Grady et al. [73] showed that DSC technique is of great value in drug purity evaluation. It is known that peak integration, according to the van't Hoff relationship, and $T_m$ values are used to test the impurities that eventually change the melting profile of a drug. However, even though the quantitative measurement of the "exact amount" of impurity of a drug is difficult, DSC is capable of monitoring the contamination and melting nature of drugs [73—75]. Because it is known that there will be a reduction in the melting temperature of a drug due to the impurities, determination of the melting temperature plays a crucial role on purity in drug [58]. DSC study of our studied compounds (Fig. 11) gave more information on these compounds by determining the melting temperatures from observed endothermic peaks and these melting point data were seen to be in consistency with the data which was previously reported to be between 238 and 240 °C for BSN-009 and 296—298 °C for BSN-011 [29]. As an ideal theoretic case, a completely pure crystalline compound should exhibit an infinitely narrow transition peak, whereas increased broadening is an indication of impurity [74]. Purity values of both compounds were also determined as 95 and 94 mol% for BSN-009 and BSN-011 by DSC and even it was suggested [76] that low scanning speed (<5 °C/min, preferably 2 °C/min) are required to determine the purity, our scanning speed was sufficient enough to determine the purities of compounds.

## 5. Conclusions

Prior determination of the molecular structure and some physicochemical characteristics of a compound and confirmation its purity are necessary steps in order it to be decided and used as a drug candidate. The most challenging issue in the pharmaceutical industry is the characterization of polymorphs of any drug or drug candidate compound. Thus, any theoretical and experimental efforts to determine the possible polymorphs/conformers of compounds are of importance. Besides, Lipinski's rule of five is used as a helpful tool in prediction of various physicochemical characteristics of the compounds as drug candidates.

Since there are not any detailed structural, spectroscopic and calorimetric data on BSN-009 and BSN-011, we performed IR, Raman, DSC and quantum chemical studies together for the first time. Our work also showed that DSC was very effective in determining the thermal behavior of BSN-009 and BSN-011. We believe that our study will pave the way to provide some predictions to design further antimicrobial/antibacterial compounds by complementary techniques as discussed and used in this work. In order to further elucidate the link between the molecular geometry and antimicrobial effects, it is obvious that new unique antimicrobial active compounds should be synthesized and compared according to their molecular structures and spectroscopic features. As a first approximation, it can be speculated that drug likeliness and bioactivity scores of BSN-011 were confirmed and this compound would be evaluated as a good drug candidate.

## Author contributions

**Ozan Unsalan:** Writing the original manuscript, review and editing. **Hatice Arı:** Theoretical calculations of the compounds, performing IR and Raman experiments, analysis of the results, preparation of tables and figures, review and editing of the paper together with Ozan Unsalan. **Cisem Altunayar-Unsalan:** Performing DSC experiments and analyses, writing DSC and IR sections, reviewing the paper. **Mustafa Boyukata:** Reviewing and editing paper, **Kayhan Bolelli:** Synthesis of the compounds, discussion of the results, writing related parts of the introduction. **Ismail Yalcin:** Synthesis of the compounds and reviewing of the paper.

## Declaration of Competing interest

All authors declare that there are no conflicts of interest to declare.

## Acknowledgements

All calculations of the present study were performed at TUBITAK ULAKBIM High Performance and Grid Computing Center (TR-Grid e-Infrastructure).

## Appendix A. Supplementary data

Supplementary data to this article can be found online at https://doi.org/10.1016/j.molstruc.2020.128454.

## References


[1] R.M. Acheson, An Introduction to the Chemistry of Heterocyclic Compounds, Interscience Publishers Inc., New York, 1960.
[2] R. Kharb, P.C. Sharma, M.S. Yar, Pharmacological significance of triazole scaffold, J. Enzym. Inhib. Med. Ch. 26 (2011) 1–21.
[3] S. Gupta, N. Ajmera, N. Gautam, R. Sharma, D.C. Gautam, Novel synthesis and biological activity study of pyrimido[2,1-b]benzothiazoles, Indian J. Chem. B. 48 (2009) 853–857.
[4] H. Kucukbay, B. Durmaz, Antifungal activity of organic and organometallic derivatives of benzimidazole and benzothiazole, Arzneimittel-Forsch. 47 (1997) 667–670.
[5] R.M. Kumbhare, V.N. Ingle, Synthesis of novel benzothiozole and benzisoxazole functionalized unsymmetrical alkanes and study of their antimicrobial activity, Indian J. Chem. B. 48 (2009) 996–1000.
[6] M.A. Mahran, S. William, F. Ramzy, A.M. Sembel, Synthesis and in vitro evaluation of new benzothiazole derivatives as schistosomicidal agents, Molecules 12 (2007) 622–633.
[7] B. Rajeeva, N. Srinivasulu, S.M. Shantakumar, Synthesis and antimicrobial activity of some new 2-substituted benzothiazole derivatives, Eur. J. Chem. 6 (2009) 775–779.
[8] G. Trapani, A. Latrofa, M. Franco, D. Armenise, F. Morlacchi, G. Liso, 3-Dihydro-1,3-Benzothiazoles, Arzneimittel-Forsch vols. 44–2 (1994) 969–971. Synthesis and Antimicrobial Activity of Some N-Alkenyl-2-Acylalkylidene-2.
[9] I. Yalcin, I. Oren, E. Sener, A. Akin, N. Ucarturk, The synthesis and the structure-activity-relationships of some substituted benzoxazoles, Oxazolo(4,5-B)Pyridines, benzothiazoles and Benzimidazoles as antimicrobial agents, Eur. J. Med. Chem. 27 (1992) 401–406.
[10] I. Yildiz-Oren, I. Yalcin, E. Aki-Sener, N. Ucarturk, Synthesis and structure-activity relationships of new antimicrobial active multi substituted benzazole derivatives, Eur. J. Med. Chem. 39 (2004) 291–298.
[11] P.H. Kalina, D.J. Shetlar, R.A. Lewis, L.J. Kullerstrand, R.F. Brubaker, 6-Amino-2-Benzothiazole-Sulfonamide - the effect of a topical carbonic-anhydrase inhibitor on Aqueous-Humor formation in the normal human-Eye, Ophthalmology 95 (1988) 772–777.
[12] M.S. Chua, D.F. Shi, S. Wrigley, T.D. Bradshaw, I. Hutchinson, P.N. Shaw, D.A. Barrett, L.A. Stanley, M.F.G. Stevens, Antitumor benzothiazoles. 7. Synthesis of 2-(4-acylaminophenyl)benzothiazoles and investigations into the role of acetylation in the antitumor activities of the parent amines, J. Med. Chem. 42 (1999) 381–392.
[13] I. Hutchinson, M.S. Chua, H.L. Browne, V. Trapani, T.D. Bradshaw, A.D. Westwell, M.F.G. Stevens, Antitumor benzothiazoles. 14. Synthesis and in vitro biological properties of fluorinated 2-(4-aminophenyl)benzothiazoles, J. Med. Chem. 44 (2001) 1446–1455.
[14] I. Hutchinson, S.A. Jennings, B.R. Vishnuvajjala, A.D. Westwell, M.F.G. Stevens, Antitumor benzothiazoles. 16. Synthesis and pharmaceutical properties of antitumor 2-(4-aminophenyl)benzothiazole amino acid prodrugs, J. Med. Chem. 45 (2002) 744–747.
[15] S. Kini, S.P. Swain, A.M. Gandhi, Synthesis and evaluation of novel benzothiazole derivatives against human cervical cancer cell lines, Indian J. of Pharmaceutical Sci. 69 (2007) 46–50.
[16] S.H.L. Kok, R. Gambari, C.H. Chui, C.W.M. Yuen, E. Lin, R.S.M. Wong, F.Y. Lau, G.Y.M. Cheng, W.S. Lam, S.H. Chan, K.H. Lam, C.H. Cheng, P.B.S. Lai, M.W.Y. Yu, F. Cheung, J.C.O. Tang, A.S.C. Chan, Synthesis and anti-cancer activity of benzothiazole containing phthalimide on human carcinoma cell lines, Bioorgan. Med. Chem. 16 (2008) 3626–3631.
[17] A. Pinar, P. Yurdakul, I. Yildiz, O. Temiz-Arpaci, N.L. Acan, E. Aki-Sener, I. Yalcin, Some fused heterocyclic compounds as eukaryotic topoisomerase II inhibitors, Biochem. Bioph. Res. Co 317 (2004) 670–674.
[18] D.F. Shi, T.D. Bradshaw, S. Wrigley, C.J. McCall, P. Lelieveld, I. Fichtner, M.F.G. Stevens, Antitumor benzothiazoles .3. Synthesis of 2-(4-aminophenyl) benzothiazoles and evaluation of their activities against breast cancer cell lines in vitro and in vivo, J. Med. Chem. 39 (1996) 3375–3384.
[19] B. Tekiner-Gulbas, O. Temiz-Arpaci, I. Yildiz, E. Aki-Sener, I. Yalcin, 3D-QSAR study on heterocyclic topoisomerase II inhibitors using CoMSIA, Sar Qsar, Environ. Res. 17 (2006) 121–132.
[20] O. Temiz-Arpaci, B. Tekiner-Gulbas, I. Yildiz, E. Aki-Sener, I. Yalcin, 3D-QSAR analysis on benzazole derivatives as eukaryotic topoisomerase II inhibitors by using comparative molecular field analysis method, Bioorgan. Med. Chem. 13 (2005) 6354–6359.
[21] M. Wang, M.Z. Gao, B.H. Mock, K.D. Miller, G.W. Sledge, G.D. Hutchins, Q.H. Zheng, Synthesis of carbon-11 labeled fluorinated 2-arylbenzothiazoles as novel potential PET cancer imaging agents, Bioorgan. Med. Chem. 14 (2006) 8599–8607.
[22] G.M. Sreenivasa, E. Jayachandran, J. Raja Kumar, M.M.J. Vijay Kumar, Synthesis of Bioactive molecule fluoro benzothiazole comprising potent heterocyclic moieties for Anthelmintic activity, Archives of Pharmacal. Res. 1 (2009) 150–157.
[23] R. Paramashivappa, P.P. Kumar, P.V.S. Rao, A.S. Rao, Design, synthesis and biological evaluation of benzimidazole/benzothiazole and benzoxazole derivatives as cyclooxygenase inhibitors, Bioorg. Med. Chem. Lett 13 (2003) 657–660.
[24] L. Katz, Antituberculous compounds. III. Benzothiazole and Bezoxazole derivatives, Journal of the Am. Chem. Soc. 75 (1953) 712–714.
[25] J. Koci, V. Klimesova, K. Waisser, J. Kaustova, H.M. Dahse, U. Mollmann, Heterocyclic benzazole derivatives with antimycobacterial in vitro activity, Bioorg. Med. Chem. Lett 12 (2002) 3275–3278.
[26] S.R. Pattan, C. Suresh, V.D. Pujar, V.V.K. Reddy, V.P. Rasal, B.C. Koti, Synthesis and antidiabetic activity of 2-amino[5 '(4-sulphonylbenzylidine)-2,4-thiazolidinedione]-7-chloro-6-fluorobenzothiazole, Indian J. Chem. B. 44 (2005) 2404–2408.
[27] K. Bolelli, I. Yalcin, T. Ertan-Bolelli, S. Ozgen, F. Kaynak-Onurdag, I. Yildiz, E. Aki, Synthesis of novel 2-[4-(4-substitutedbenzamido/phenylacetamido) phenyl]benzothiazoles as antimicrobial agents, Med. Chem. Res. 21 (2012) 3818–3825.
[28] I. Yalcin, B.K. Kaymakcioglu, I. Oren, E. Sener, O. Temiz, A. Akin, N. Altanlar, Synthesis and microbiological activity of some novel N-(2-hydroxyl-5-substitutedphenyl)benzacetamides, phenoxyacetamides and thiophenoxyacetamides as the possible metabolites of antimicrobial active benzoxazoles, Farmaco 52 (1997) 685–689.
[29] S. Yilmaz, I. Yalcin, F. Kaynak-Onurdag, S. Ozgen, I. Yildiz, E. Aki, Synthesis and in vitro antimicrobial activity of novel 2-(4-(Substituted-carboxamido)benzyl/phenyl)benzothiazoles, Croat. Chem. Acta 86 (2013) 223–231.
[30] F. Billes, H. Pataki, O. Unsalan, H. Mikosch, B. Vajna, G. Marosi, Solvent effect on the vibrational spectra of Carvedilol, Spectrochim. Acta A. 95 (2012) 148–164.
[31] Y. Erdogdu, O. Dereli, D. Sajan, L. Joseph, O. Unsalan, M.T. Gulluoglu, Vibrational (FT-IR and FT-Raman) spectral investigations of 7-aminoflavone with density functional theoretical simulations, Mol. Simulat. 38 (2012) 315–325.
[32] Y. Erdogdu, O. Unsalan, M. Amalanathan, I.H. Joe, Infrared and Raman spectra, vibrational assignment, NBO analysis and DFT calculations of 6-aminoflavone, J. Mol. Struct. 980 (2010) 24–30.
[33] Y. Erdogdu, O. Unsalan, M.T. Gulluoglu, Ft-Raman, FT-IR spectral and DFT studies on 6, 8-dichloroflavone and 6, 8-dibromoflavone, J. Raman. Spec. 41 (2010) 820–828.
[34] Y. Erdogdu, O. Unsalan, D. Sajan, M.T. Gulluoglu, Structural conformations and vibrational spectral study of chloroflavone with density functional theoretical simulations, Spectrochim. Acta 76 (2010) 130–136.
[35] O. Unsalan, Y. Erdogdu, M.T. Gulluoglu, FT-Raman and FT-IR spectral and quantum chemical studies on some flavonoid derivatives: Baicalein and Naringenin, J. Raman Spec. 40 (2009) 562–570.
[36] O. Unsalan, N. Kus, S. Jarmelo, R. Faust, Trans- and cis-stilbene isolated in cryogenic argon and xenon matrices, Spectrochim. Acta A. 136 (2015) 81–94.
[37] O. Unsalan, Y. Sert, H. Ari, A. Simao, A. Yilmaz, M. Boyukata, O. Bolukbasi, K. Bolelli, I. Yalcin, Micro-Raman, Mid-IR, Far-IR and DFT studies on 2-[4-(4-Fluorobenzamido)phenyl]benzothiazole, Spectrochim. Acta 125 (2014) 414–421.
[38] O. Unsalan, B. Szolnoki, A. Toldy, G. Marosi, FT-IR spectral, DFT studies and detailed vibrational assignment on N,N ',N ''-tris(2-aminoethyl)-phosphoric acid triamide, Spectrochim. Acta A. 98 (2012) 110–115.
[39] O. Unsalan, A. Tutar, C.S. Unlu, R. Erenler, FTIR spectroscopic and quantum-chemical studies on some tribromoindenes and their isomers, Opt. Spectrosc. 111 (2011) 894–903.
[40] M. Govindarajan, A.S. Abdelhameed, A.A. Al-Saadi, M.I. Attia, Experimental and theoretical studies of the vibrational and electronic properties of (2E)-2-[3-(1H-imidazole-1-yl)-1-phenyl-propylidene]-N-phenyl-hydrazinecarboxamide: an anticonvulsant agent, Appl. Sci-Basel. 5 (2015) 955–972.
[41] J. Binoy, I.H. Joe, V.S. Jayakumar, O.F. Nielsen, J. Aubard, DFT based relaxed PES scan studies and SERS of anti cancer drug, Combretastatin A-4, Laser Phys. Lett. 2 (2005) 544–550.
[42] M. Torres, S. Khan, M. Duplanty, H.C. Lozano, T.J. Morris, T. Nguyen, Y.V. Rostovtsev, N.J. DeYonker, N. Mirsaleh-Kohan, Raman and Infrared studies of platinum-based drugs: cisplatin, carboplatin, oxaliplatin, nedaplatin, and heptaplatin, J. Phys. Chem. A. 122 (2018) 6934–6952.
[43] D.M. Sena, P.T.C. Freire, J. Mendes, F.E.A. Melo, F.M. Pontes, E. Longo, O.P. Ferreira, O.L. Alves, Vibrational and thermal properties of crystalline topiramate, J. Brazil Chem. Soc. 19 (2008) 1607–1613.
[44] S. Singh, H. Singh, T. Karthick, P. Tandon, D.H. Dethe, R.D. Erande, Conformational study and vibrational spectroscopic (FT-IR and FT-Raman) analysis of an Alkaloid-borreverine derivative, Anal. Sci. 33 (2017) 99–104.
[45] A. Borrego-Sanchez, E. Carazo, B. Albertini, N. Passerini, B. Perissutti, P. Cerezo, C. Viseras, A. Hernandez-Laguna, C. Aguzzi, C.I. Sainz-Diaz, Conformational polymorphic changes in the crystal structure of the chiral antiparasitic drug praziquantel and interactions with calcium carbonate, Eur. J. Pharm. Biopharm. 132 (2018) 180–191.
[46] C. Fandaruff, G.S. Rauber, A.M. Araya-Sibaja, R.N. Pereira, C.E.M. de Campos, H.V.A. Rocha, G.A. Monti, T. Malaspina, M.A.S. Silva, S.L. Cuffini, Polymorphism of anti-HIV drug Efavirenz: investigations on thermodynamic and Dissolution properties, Cryst. Growth Des. 14 (2014) 4968–4975.
[47] M.A.L. Pinto, B. Ambrozini, A.P.G. Ferreira, E.T.G. Cavalheiro, Thermoanalytical studies of carbamazepine: hydration/dehydration, thermal decomposition, and solid phase transitions, Braz. J. Pharm. Sci. 50 (2014) 877–884.

[48] Ali K. Attia, Mona M. Abdel-Moety, Samar G. Abdel-Hamid, Thermal analysis study of antihypertensive drug doxazosin mesilate, Arabian J. Chem. 10 (2012) 334–338.
[49] L.F.A. Romani, M.I. Yoshida, E.C.L. Gomes, R.R. Machado, F.F. Rodrigues, M.M. Coelho, M.A. Oliveira, M.B. Freitas-Marques, R.A.S. San Gil, W.N. Mussel, Physicochemical characterization, the Hirshfeld surface, and biological evaluation of two meloxicam compounding pharmacy samples, J. Pharm. Anal. 8 (2018) 103–108.
[50] V. Arjunan, S.T. Govindaraja, S.P. Jose, S. Mohan, DFT simulation, quantum chemical electronic structure, spectroscopic and structure-activity investigations of 2-benzothiazole acetonitrile, Spectrochim. Acta 128 (2014) 22–36.
[51] A.S. Devi, V.V. Aswathy, Y.S. Mary, C.Y. Panicker, S. Armakovic, S.J. Armakovic, R. Ravindran, C. Van Alsenoy, Synthesis, XRD single crystal structure analysis, vibrational spectral analysis, molecular dynamics and molecular docking studies of 2-(3-methoxy-4-hydroxyphenyl) benzothiazole, J. Mol. Struct. 1148 (2017) 282–292.
[52] E. Koglin, E.G. Witte, R.J. Meier, The vibrational spectra of metabolites of methabenzthiazuron: 2-amino-benzothiazole and 2-(methylamino)benzothiazole, Vib. Spec. 33 (2003) 49–61.
[53] W. Li, Q.F. Wu, Y. Ye, M.D. Luo, L. Hu, Y.H. Gu, F. Niu, J.M. Hu, Density functional theory and ab initio studies of geometry, electronic structure and vibrational spectra of novel benzothiazole and benzotriazole herbicides, Spectrochim. Acta 60 (2004) 2343–2354.
[54] U. Pandey, M. Srivastava, R.P. Singh, R.A. Yadav, DFT study of conformational and vibrational characteristics of 2-(2-hydroxyphenyl)benzothiazole molecule, Spectrochim. Acta 129 (2014) 61–73.
[55] D. Romani, S.A. Brandan, Structural and spectroscopic studies of two 1,3-benzothiazole tautomers with potential antimicrobial activity in different media. Prediction of their reactivities, Comput. Theor. Chem. 1061 (2015) 89–99.
[56] V. Sathyanarayanmoorthi, R. Karunathan, V. Kannappan, Molecular modeling and spectroscopic studies of benzothiazole, J. Chem-Ny, 2013, pp. 1–14.
[57] R. Sun, J.L. Yao, S.J. Li, R.N. Gu, Raman spectroscopic and density functional theory studies on a benzothiazole-2-thione derivative, Vib. Spectrosc. 47 (2008) 38–43.
[58] L. Bond, S. Allen, M.C. Davies, C.J. Roberts, A.P. Shivji, S.J.B. Tendler, P.M. Williams, J.X. Zhang, Differential scanning calorimetry and scanning thermal microscopy analysis of pharmaceutical materials, Int. J. Pharmaceut. 243 (2002) 71–82.
[59] M.J. Frisch, G.W. Trucks, H.B. Schlegel, G.E. Scuseria, M.A. Robb, J.R. Cheeseman, G. Scalmani, V. Barone, B. Mennucci, G.A. Petersson, H. Nakatsuji, M. Caricato, X. Li, H.P. Hratchian, A.F. Izmaylov, J. Bloino, G. Zheng, J.L. Sonnenberg, M. Hada, M. Ehara, K. Toyota, R. Fukuda, J. Hasegawa, M. Ishida, T. Nakajima, Y. Honda, O. Kitao, H. Nakai, T. Vreven, J.A. Montgomery Jr., J.E. Peralta, F. Ogliaro, M. Bearpark, J.J. Heyd, E. Brothers, K.N. Kudin, V.N. Staroverov, T. Keith, R. Kobayashi, J. Normand, K. Raghavachari, A. Rendell, J.C. Burant, S.S. Iyengar, J. Tomasi, M. Cossi, N. Rega, J.M. Millam, M. Klene, J.E. Knox, J.B. Cross, V. Bakken, C. Adamo, J. Jaramillo, R. Gomperts, R.E. Stratmann, O. Yazyev, A.J. Austin, R. Cammi, C. Pomelli, J.W. Ochterski, R.L. Martin, K. Morokuma, V.G. Zakrzewski, G.A. Voth, P. Salvador, J.J. Dannenberg, S. Dapprich, A.D. Daniels, O. Farkas, J.B. Foresman, J.V. Ortiz, J. Cioslowski, D.J. Fox, Gaussian 09, Revision B.01, 2010.
[60] Roy D. Dennington, Todd A. Keith, J. Millam, GaussView, Version 5, Semichem Inc, Shawnee Mission KS, 2009.
[61] M.H. Jamroz, Vibrational energy distribution analysis (VEDA): Scopes and limitations, Spectrochim. Acta A. 114 (2013) 220–230.
[62] E. Kavitha, N. Sundaraganesan, S. Sebastian, M. Kurt, Molecular structure, anharmonic vibrational frequencies and NBO analysis of naphthalene acetic acid by density functional theory calculations, Spectrochim. Acta A. 77 (2010) 612–619.
[63] T. Koopmans, Über die Zuordnung von Wellenfunktionen und Eigenwerten zu den Einzelnen Elektronen Eines Atoms, Phys. Rev. C 1 (1934) 104–113.
[64] R.S. Mulliken, Electronic Population analysis on LCAO–MO molecular Wave functions. I, J. Chem. Phys. 23 (1955) 1833–1840.
[65] P. Govindasamy, S. Gunasekaran, Spectroscopic (FT-IR, FT-Raman and UV) investigation, NLO, NBO, molecular orbital and MESP analysis of 2-{2-[(2,6-dichlorophenyl)amino]phenyl}acetic acid, Spectrochim. Acta 136 Pt (2015) 1543–1556.
[66] C.A. Lipinski, F. Lombardo, B.W. Dominy, P.J. Feeney, Experimental and computational approaches to estimate solubility and permeability in drug discovery and development settings, Adv Drug Deliver. Rev. 64 (2012) 4–17.
[67] C.A. Lipinski, F. Lombardo, B.W. Dominy, P.J. Feeney, Experimental and computational approaches to estimate solubility and permeability in drug discovery and development settings (Reprinted from Advanced Drug Delivery Reviews, vol 23, pg 3-25, 1997), Adv. Drug Deliver. Rev. 46 (2001) 3–26.
[68] C.A. Lipinski, F. Lombardo, B.W. Dominy, P.J. Feeney, Experimental and computational approaches to estimate solubility and permeability in drug discovery and development settings, Adv. Drug Deliver Rev. 23 (1997) 3–25.
[69] Molinspiration Cheminformatics, 2020. https://www.molinspiration.com/cgi-bin/properties.
[70] N.M. O'Boyle, M. Banck, C.A. James, C. Morley, T. Vandermeersch, G.R. Hutchison, Open Babel: an open chemical toolbox, J. of Cheminformatics. 3 (2011) 33, 2011.
[71] D.F. Veber, S.R. Johnson, H.Y. Cheng, B.R. Smith, K.W. Ward, K.D. Kopple, Molecular properties that influence the oral bioavailability of drug candidates, J. Med. Chem. 45 (2002) 2615–2623.
[72] Noël P.G. Roeges, A Guide to the Complete Interpretation of Infrared Spectral of Organic Structures, Wiley, Chichester, 1994, pp. 1–356.
[73] L.T. Grady, S.E. Hays, R.H. King, H.R. Klein, W.J. Mader, D.K. Wyatt, R.O. Zimmerer Jr., Drug purity profiles, J. Pharm. Sci-Us 62 (1973) 456–464.
[74] A.A. Vandooren, B.W. Muller, Purity determinations of drugs with Differential scanning calorimetry (Dsc) - a Critical-review, Int. J. Pharmaceut. 20 (1984) 217–233.
[75] Michael H. Chiu, Elmar J. Prenner, Differential scanning calorimetry: an invaluable tool for a detailed thermodynamic characterization of macromolecules and their interactions, J. of Pharmacy and Bioallied Sciences 3 (2011) 39–59.
[76] S.D. Clas, C.R. Dalton, B.C. Hancock, Differential scanning calorimetry: applications in drug development, Pharm. Sci. Technol. To. 2 (1999) 311–320.